

A posteriori error analyses of a velocity-pseudostress formulation of the generalized Stokes problem

TOMÁS P. BARRIOS*, ROMMEL BUSTINZA†, GALINA C. GARCÍA‡,
and MARÍA GONZÁLEZ§

Abstract

We develop two a posteriori error analyses for an augmented mixed method for the generalized Stokes problem. The stabilized scheme is obtained by adding suitable least squares terms to the velocity-pseudostress formulation of the generalized Stokes problem. Then, in order to approximate its solution applying an adaptive mesh refinement technique, we derive two reliable a posteriori error estimators of residual type, and study their efficiency. To this aim, we include two different analyses: the standard residual based approach and an unusual one based on the Ritz projection of the error. The main difference of both approaches relies on the way we treat the nonhomogeneous boundary condition. Finally, we present some numerical examples that confirm the theoretical properties of our approach and estimators.

Mathematics Subject Classifications (1991): 65N15, 65N30, 65N50, 76D07

Key words: Generalized Stokes problem, velocity-pseudostress formulation, a posteriori error estimator.

1 Introduction

It is well-known that the so-called generalized Stokes problem plays a fundamental role in the numerical simulation of viscous incompressible flows (both laminar and turbulent). This

*Departamento de Matemática y Física Aplicadas, Universidad Católica de la Santísima Concepción, Casilla 297, Concepción, Chile, email: tomas@ucsc.cl

†Departamento de Ingeniería Matemática & Centro de Investigación en Ingeniería Matemática (CIM²A), Universidad de Concepción, Casilla 160-C, Concepción, Chile, email: rbustinz@ing-mat.udec.cl

‡Departamento de Matemática y Ciencia de la Computación, Universidad de Santiago de Chile, Casilla 307, Correo 2, Santiago, Chile, email: galina.garcia@usach.cl

§Departamento de Matemáticas, Universidad de A Coruña, Campus de Elviña s/n, 15071, A Coruña, Spain, e-mail: maria.gonzalez.taboada@udc.es

model appears, for instance, when the nonlinear term in a time discretization of the Navier-Stokes equations is evaluated explicitly and an implicit scheme is used for the linear part. This fact produced increasing efforts to study the numerical approximation of the generalized Stokes problem by different techniques (see, for e.g. [2],[4],[8],[9],[11],[20],[21], and the references therein). Concerning the standard velocity-pressure variational formulation of the problem, a nonoverlapping domain decomposition approach is developed in [11] with the aim to obtain a parallel solver; different stabilization techniques can be found in [4] and [8]; and adaptive solution is studied at least in [20], [21] and [2]. On the other hand, a dual-mixed method obtained after including the flux and the tensor gradient of the velocity as additional unknowns, is introduced and analyzed in [9], where an a posteriori error analysis, based on local problems, is also developed.

More recently, the so-called velocity-pseudostress formulation was introduced in [10] (see also [17]) for the stationary Stokes problem, and a stabilized scheme was developed in [18]. In the framework of the generalized Stokes problem, dual-mixed methods based on the pseudostress are studied in [16] and [5]. In [16] the velocity is eliminated from the formulation while in [5] an augmented dual-mixed method is proposed.

Now, in order to describe the model of interest, we let Ω be a bounded open subset of \mathbb{R}^2 with Lipschitz continuous boundary Γ . Then, given the source term $\mathbf{f} \in [L^2(\Omega)]^2$ and $\mathbf{g} \in [H^{1/2}(\Gamma)]^2$, we look for the velocity \mathbf{u} and the pressure p of the fluid occupying the region Ω , such that

$$\begin{cases} \alpha\mathbf{u} - \nu\Delta\mathbf{u} + \nabla p = \mathbf{f} & \text{in } \Omega, \\ \operatorname{div}(\mathbf{u}) = 0 & \text{in } \Omega, \\ \mathbf{u} = \mathbf{g} & \text{on } \Gamma, \end{cases} \quad (1)$$

where ν is the kinematic viscosity of the fluid, that we assume constant, α is a positive parameter proportional to the inverse of the time-step and the datum \mathbf{g} satisfies the compatibility condition $\int_{\Gamma} \mathbf{g} \cdot \mathbf{n} = 0$, where \mathbf{n} stands for the unit outward normal to Γ . In addition, in order to guarantee uniqueness, we assume that the pressure $p \in L_0^2(\Omega) := \{q \in L^2(\Omega) : \int_{\Omega} q = 0\}$.

Motivated by the competitive character of the velocity-pseudostress formulation introduced in [5], our interest now is to develop an a posteriori error analysis and then implement an adaptive algorithm to approximate the solution of (1). The rest of the paper is organized as follows. In Section 2, we recall the velocity-pseudostress formulation introduced in Remark 3.1 in [5], and restate the existence and uniqueness result. Next, in Section 3, we derive an a posteriori error estimator of residual type following the standard approach. In Section 4, an unusual a posteriori error estimator based on the Ritz projection is obtained and analyzed. Finally, numerical examples including a comparison of the behavior of both estimators are reported in Section 5.

We end this section with some notations to be used throughout the paper. Given any Hilbert space H , we denote by H^2 the space of vectors of order 2 with entries in H , and by

$H^{2 \times 2}$ the space of square tensors of order 2 with entries in H . In particular, given $\boldsymbol{\tau} := (\tau_{ij})$, $\boldsymbol{\zeta} := (\zeta_{ij}) \in \mathbb{R}^{2 \times 2}$, we write, as usual, $\boldsymbol{\tau}^t := (\tau_{ji})$, $\text{tr}(\boldsymbol{\tau}) := \tau_{11} + \tau_{22}$, $\boldsymbol{\tau}^d := \boldsymbol{\tau} - \frac{1}{2}\text{tr}(\boldsymbol{\tau})\mathbf{I}$ and $\boldsymbol{\tau} : \boldsymbol{\zeta} := \sum_{i,j=1}^2 \tau_{ij} \zeta_{ij}$, where \mathbf{I} is the identity matrix in $\mathbb{R}^{2 \times 2}$. We also use the standard notations for Sobolev spaces and norms. We denote by $H_0 := \{\boldsymbol{\tau} \in H(\mathbf{div}; \Omega) : \int_{\Omega} \text{tr}(\boldsymbol{\tau}) = 0\}$. We recall that $H(\mathbf{div}; \Omega) = H_0 \oplus \mathbb{R}\mathbf{I}$, that is, for any $\boldsymbol{\tau} \in H(\mathbf{div}; \Omega)$ there exists a unique $\boldsymbol{\tau}_0 \in H_0$ and $d := \frac{1}{2|\Omega|} \int_{\Omega} \text{tr}(\boldsymbol{\tau}) \in \mathbb{R}$ such that $\boldsymbol{\tau} = \boldsymbol{\tau}_0 + d\mathbf{I}$. Finally, we use C or c , with or without subscripts, to denote generic constants, independent of the mesh size, which may take different values at different occurrences.

2 The stabilized mixed formulation

In this section we describe the stabilized mixed variational formulation introduced in Remark 3.1 in [5]. First, the so-called pseudostress $\boldsymbol{\sigma} := \nu \nabla \mathbf{u} - p\mathbf{I}$ in Ω is introduced, and proceeding as in [5], we derive to a variational formulation that reads as: Find $(\boldsymbol{\sigma}, \mathbf{u}) \in \mathbf{H}_0 := H_0 \times [H^1(\Omega)]^2$ such that

$$a((\boldsymbol{\sigma}, \mathbf{u}), (\boldsymbol{\tau}, \mathbf{v})) = F(\boldsymbol{\tau}, \mathbf{v}) \quad \forall (\boldsymbol{\tau}, \mathbf{v}) \in \mathbf{H}_0, \quad (2)$$

where the bilinear form $a : \mathbf{H}_0 \times \mathbf{H}_0 \rightarrow \mathbb{R}$, and the linear functional $F : \mathbf{H}_0 \rightarrow \mathbb{R}$ are defined by

$$\begin{aligned} a((\boldsymbol{\zeta}, \mathbf{w}), (\boldsymbol{\tau}, \mathbf{v})) &:= \int_{\Omega} \boldsymbol{\zeta}^d : \boldsymbol{\tau}^d + \nu \int_{\Omega} \mathbf{w} \cdot \mathbf{div}(\boldsymbol{\tau}) - \nu \int_{\Omega} \mathbf{v} \cdot \mathbf{div}(\boldsymbol{\zeta}) + \alpha \nu \int_{\Omega} \mathbf{w} \cdot \mathbf{v} \\ &\quad + \kappa_1 \int_{\Omega} (\nu \nabla \mathbf{w} - \boldsymbol{\zeta}^d) : \nabla \mathbf{v} + \kappa_2 \int_{\Omega} (\mathbf{div}(\boldsymbol{\zeta}) - \alpha \mathbf{w}) \cdot \mathbf{div}(\boldsymbol{\tau}) \end{aligned} \quad (3)$$

and

$$F(\boldsymbol{\tau}, \mathbf{v}) := \nu \int_{\Omega} \mathbf{f} \cdot \mathbf{v} + \nu \int_{\Gamma} \mathbf{g} \cdot \boldsymbol{\tau} \mathbf{n} - \kappa_2 \int_{\Omega} \mathbf{f} \cdot \mathbf{div}(\boldsymbol{\tau}), \quad (4)$$

for any $(\boldsymbol{\zeta}, \mathbf{w}), (\boldsymbol{\tau}, \mathbf{v}) \in \mathbf{H}_0$, where κ_1 and κ_2 are unknown positive parameters.

The well posedness of problem (2) follows from the Lax-Milgram Lemma, and requires the following result.

Lemma 2.1 *There exists $c_1 \in]0, 1]$ such that*

$$c_1 \|\boldsymbol{\tau}\|_{[L^2(\Omega)]^{2 \times 2}}^2 \leq \|\boldsymbol{\tau}^d\|_{[L^2(\Omega)]^{2 \times 2}}^2 + \|\mathbf{div}(\boldsymbol{\tau})\|_{[L^2(\Omega)]^2}^2, \quad \forall \boldsymbol{\tau} \in H_0.$$

Proof. See proof of Proposition IV.3.1 in [7]. □

Next, we establish the ellipticity of the bilinear form $a(\cdot, \cdot)$.

Lemma 2.2 Let $\kappa_1 \in (0, 2\nu)$ and $\kappa_2 \in (0, 2\nu/\alpha)$. Then, there exists a positive constant C_{ell} such that

$$a((\boldsymbol{\tau}, \mathbf{v}), (\boldsymbol{\tau}, \mathbf{v})) \geq C_{ell} \|(\boldsymbol{\tau}, \mathbf{v})\|_{\mathbf{H}_0}^2, \quad \forall (\boldsymbol{\tau}, \mathbf{v}) \in \mathbf{H}_0.$$

Proof. Let $(\boldsymbol{\tau}, \mathbf{v}) \in \mathbf{H}_0$. Then, from the proof of Lemma 3.2 in [5] we know that

$$\begin{aligned} a((\boldsymbol{\tau}, \mathbf{v}), (\boldsymbol{\tau}, \mathbf{v})) &\geq \left(1 - \frac{\kappa_1}{2}\epsilon_1\right) \|\boldsymbol{\tau}^d\|_{[L^2(\Omega)]^{2 \times 2}}^2 + \alpha \left(\nu - \frac{\kappa_2}{2}\epsilon_2\right) \|\mathbf{v}\|_{[L^2(\Omega)]^2}^2 \\ &+ \kappa_1 \left(\nu - \frac{1}{2\epsilon_1}\right) |\mathbf{v}|_{[H^1(\Omega)]^2}^2 + \kappa_2 \left(1 - \frac{\alpha}{2\epsilon_2}\right) \|\operatorname{div}(\boldsymbol{\tau})\|_{[L^2(\Omega)]^2}^2. \end{aligned}$$

Taking $\epsilon_1 = 1/\nu$ and $\epsilon_2 = \alpha$, we have that

$$\begin{aligned} a((\boldsymbol{\tau}, \mathbf{v}), (\boldsymbol{\tau}, \mathbf{v})) &\geq \left(1 - \frac{\kappa_1}{2\nu}\right) \|\boldsymbol{\tau}^d\|_{[L^2(\Omega)]^{2 \times 2}}^2 + \alpha \left(\nu - \frac{\kappa_2}{2}\alpha\right) \|\mathbf{v}\|_{[L^2(\Omega)]^2}^2 \\ &+ \kappa_1 \frac{\nu}{2} |\mathbf{v}|_{[H^1(\Omega)]^2}^2 + \frac{\kappa_2}{2} \|\operatorname{div}(\boldsymbol{\tau})\|_{[L^2(\Omega)]^2}^2. \end{aligned}$$

Now, for $\kappa_1 \in (0, 2\nu)$ and $\kappa_2 \in (0, 2\nu/\alpha)$, it is clear that

$$1 - \frac{\kappa_1}{2\nu} > 0 \quad \text{and} \quad \nu - \frac{\kappa_2}{2}\alpha > 0,$$

and applying Lemma 2.1, the proof follows. \square

We remark that for the feasible choice $\kappa_1 = \nu$ and $\kappa_2 = \nu/\alpha$, we obtain that

$$\begin{aligned} a((\boldsymbol{\tau}, \mathbf{v}), (\boldsymbol{\tau}, \mathbf{v})) &\geq \frac{1}{2} \|\boldsymbol{\tau}^d\|_{[L^2(\Omega)]^{2 \times 2}}^2 + \alpha \frac{\nu}{2} \|\mathbf{v}\|_{[L^2(\Omega)]^2}^2 + \frac{\nu^2}{2} |\mathbf{v}|_{[H^1(\Omega)]^2}^2 + \frac{\nu}{2\alpha} \|\operatorname{div}(\boldsymbol{\tau})\|_{[L^2(\Omega)]^2}^2 \\ &\geq c_1 \min\left\{\frac{1}{2}, \frac{\nu}{4\alpha}\right\} \|\boldsymbol{\tau}\|_{[L^2(\Omega)]^{2 \times 2}}^2 + \frac{\nu}{4\alpha} \|\operatorname{div}(\boldsymbol{\tau})\|_{[L^2(\Omega)]^2}^2 + \frac{1}{2} \min\{\alpha\nu, \nu^2\} \|\mathbf{v}\|_{[H^1(\Omega)]^2}^2 \\ &\geq \frac{1}{2} \min\left\{c_1, \frac{\nu c_1}{2\alpha}, \alpha\nu, \nu^2\right\} \|(\boldsymbol{\tau}, \mathbf{v})\|_{\mathbf{H}_0}^2. \end{aligned}$$

Thus we note, in this particular case, that $C_{ell} := \frac{1}{2} \min\{c_1, \frac{\nu c_1}{2\alpha}, \alpha\nu, \nu^2\}$. In particular, if $\alpha \leq \nu$ we obtain that $C_{ell} := \frac{1}{2} \min\{\frac{c_1}{2}, \alpha\nu\}$, from which we deduce that $C_{ell} = \mathcal{O}(\alpha)$ for $\alpha \ll \nu \leq 1$. Moreover, for $\alpha > \nu$, we deduce $C_{ell} := \frac{c_1\nu}{4\alpha} \in]0, 1[$ if $\nu \geq 1$, and $C_{ell} := \frac{1}{2} \min\{\frac{c_1\nu}{2\alpha}, \nu^2\} \in]0, 1[$ if $\nu < 1$. Both cases imply that $C_{ell} = \mathcal{O}(\frac{1}{\alpha})$ for $\alpha \gg \nu \geq 1$.

Now we describe the Galerkin scheme associated to the continuous problem (2). Hereafter, we assume that the parameters κ_1 and κ_2 satisfy the assumptions of Lemma 2.2. In addition, we suppose that Ω is a polygonal region and h is a positive parameter. We consider finite element subspaces $H_{0,h}^\sigma \subset H_0$ and $H_h^u \subset [H^1(\Omega)]^2$. Then, a Galerkin scheme associated to the variational problem (2) reads: Find $(\boldsymbol{\sigma}_h, \mathbf{u}_h) \in \mathbf{H}_{0,h} := H_{0,h}^\sigma \times H_h^u$ such that

$$a((\boldsymbol{\sigma}_h, \mathbf{u}_h), (\boldsymbol{\tau}_h, \mathbf{v}_h)) = F(\boldsymbol{\tau}_h, \mathbf{v}_h), \quad \forall (\boldsymbol{\tau}_h, \mathbf{v}_h) \in \mathbf{H}_{0,h}. \quad (5)$$

The well-posedness of the discrete problem (5) follows from the Lax-Milgram Lemma.

In order to describe a particular finite element subspace $\mathbf{H}_{0,h}$, we let $\{\mathcal{T}_h\}_{h>0}$ be a regular family of triangulations of $\bar{\Omega} = \cup\{T : T \in \mathcal{T}_h\}$ and, given a triangle $T \in \mathcal{T}_h$, we denote by h_T its diameter and define the mesh size $h := \max\{h_T : T \in \mathcal{T}_h\}$. In addition, given an integer $\ell \geq 0$ and a subset S of \mathbb{R}^2 , we denote by $\mathcal{P}_\ell(S)$ the space of polynomials in two variables defined in S of total degree at most ℓ , and for each $T \in \mathcal{T}_h$, we define the local Raviart-Thomas space of the lowest order

$$\mathcal{RT}_0(T) := \text{span} \left\{ \begin{pmatrix} 1 \\ 0 \end{pmatrix}, \begin{pmatrix} 0 \\ 1 \end{pmatrix}, \begin{pmatrix} x_1 \\ x_2 \end{pmatrix} \right\} \subseteq [\mathcal{P}_1(T)]^2,$$

where $\begin{pmatrix} x_1 \\ x_2 \end{pmatrix}$ is a generic vector of \mathbb{R}^2 .

Then we define

$$H_h^\sigma := \left\{ \boldsymbol{\tau}_h \in H(\mathbf{div}; \Omega) : \boldsymbol{\tau}_h|_T \in [\mathbb{RT}_0(T)]^2 \quad \forall T \in \mathcal{T}_h \right\},$$

$$H_{0,h}^\sigma := \left\{ \boldsymbol{\tau}_h \in H_h^\sigma : \int_\Omega \text{tr}(\boldsymbol{\tau}_h) = 0 \right\}, \quad (6)$$

$$X_h := \left\{ v_h \in \mathcal{C}(\bar{\Omega}) : v_h|_T \in \mathcal{P}_1(T) \quad \forall T \in \mathcal{T}_h \right\}, \quad (7)$$

and

$$H_h^u := X_h \times X_h. \quad (8)$$

Next, we give the rate of convergence of the Galerkin scheme (5) when the finite element subspace $\mathbf{H}_{0,h} := H_{0,h}^\sigma \times H_h^u$ is used, with $H_{0,h}^\sigma$ and H_h^u defined by (6) and (8), respectively.

Theorem 2.1 *Let $(\boldsymbol{\sigma}, \mathbf{u}) \in \mathbf{H}_0$ and $(\boldsymbol{\sigma}_h, \mathbf{u}_h) \in \mathbf{H}_{0,h}$ be the unique solutions of the continuous and discrete augmented mixed formulations (2) and (5), respectively. Assume that $\boldsymbol{\sigma} \in [H^r(\Omega)]^{2 \times 2}$, $\mathbf{div}(\boldsymbol{\sigma}) \in [H^r(\Omega)]^2$ and $\mathbf{u} \in [H^{r+1}(\Omega)]^2$, for some $r \in (0, 1]$. Then, there exists $C_{roc} > 0$, independent of h , such that*

$$\|(\boldsymbol{\sigma}, \mathbf{u}) - (\boldsymbol{\sigma}_h, \mathbf{u}_h)\|_{\mathbf{H}_0} \leq C_{roc} h^r \left\{ \|\boldsymbol{\sigma}\|_{[H^r(\Omega)]^{2 \times 2}} + \|\mathbf{div}(\boldsymbol{\sigma})\|_{[H^r(\Omega)]^2} + \|\mathbf{u}\|_{[H^{r+1}(\Omega)]^2} \right\}.$$

Proof. The proof follows from the classical Céa estimate and the corresponding approximation properties of the finite element subspaces. \square

In order to describe the behavior of the constant C_{roc} , we first note that, there exists $M > 0$ such that

$$|a((\boldsymbol{\tau}, \mathbf{v}), (\boldsymbol{\zeta}, \mathbf{w}))| \leq M \|(\boldsymbol{\tau}, \mathbf{v})\|_{\mathbf{H}_0} \|(\boldsymbol{\zeta}, \mathbf{w})\|_{\mathbf{H}_0}.$$

It is not difficult to see that $M := 1 + 2\nu + \alpha\nu + \kappa_1(1 + \nu) + \kappa_2(1 + \alpha)$ holds the above inequality. In particular, for the choice $\kappa_1 = \nu$ and $\kappa_2 = \nu/\alpha$, we deduce $M := 1 + 4\nu + \alpha\nu + \nu^2 + \frac{\nu}{\alpha}$, which implies that $M = \mathcal{O}(\alpha)$ if $\alpha \gg \nu \geq 1$. Then, using that for this case, it is well known that the characterization of the constant is given by $C_{roc} := \frac{M}{C_{ell}}$, we note in particular that $C_{roc} = \mathcal{O}(\alpha^2)$ if $\alpha \gg \nu \geq 1$.

3 A residual-based a posteriori error analysis

In this section we develop a residual-based a posteriori error analysis for the augmented finite element scheme (5). We first introduce some notations and results concerning the Clément and Raviart-Thomas interpolation operators.

3.1 Some notation and preliminary results

Given $T \in \mathcal{T}_h$, we let $E(T)$ be the set of its edges, and let E_h be the set of all edges induced by the triangulation \mathcal{T}_h . Then, we write $E_h = E_I \cup E_\Gamma$, where $E_I := \{e \in E_h : e \subseteq \Omega\}$ and $E_\Gamma := \{e \in E_h : e \subseteq \Gamma\}$. Also, for each edge $e \in E_h$, we fix a unit normal vector $\mathbf{n}_e := (n_1, n_2)^\top$, and let $\mathbf{t}_e := (-n_2, n_1)^\top$ be the corresponding fixed unit tangential vector along e . From now on, when no confusion arises, we simply write \mathbf{n} and \mathbf{t} instead of \mathbf{n}_e and \mathbf{t}_e , respectively. Finally, given a vector valued field $\mathbf{v} := (v_1, v_2)^\top$, we denote

$$\underline{\text{curl}}(\mathbf{v}) := \begin{pmatrix} \frac{\partial v_1}{\partial x_2} & -\frac{\partial v_1}{\partial x_1} \\ \frac{\partial v_2}{\partial x_2} & -\frac{\partial v_2}{\partial x_1} \end{pmatrix}.$$

We will use the Clément interpolation operator $I_h : H^1(\Omega) \rightarrow X_h$ (cf. [14]). A vector version of this operator, say $\mathbf{I}_h : [H^1(\Omega)]^2 \rightarrow H_h^\mathbf{u}$, is defined component-wise by I_h . The following lemma establishes the local approximation properties of I_h .

Lemma 3.1 *There exist constants $c_1, c_2 > 0$, independent of h , such that for all $v \in H^1(\Omega)$ there holds*

$$\|v - I_h(v)\|_{H^m(T)} \leq c_1 h_T^{1-m} \|v\|_{H^1(\omega(T))}, \quad \forall m \in \{0, 1\}, \forall T \in \mathcal{T}_h,$$

and

$$\|v - I_h(v)\|_{L^2(e)} \leq c_2 h_e^{1/2} \|v\|_{H^1(\omega(e))} \quad \forall e \in E_h,$$

where $\omega(T) := \cup\{T' \in \mathcal{T}_h : T' \cap T \neq \emptyset\}$, h_e denote the length of the side $e \in E_h$ and $\omega(e) := \cup\{T' \in \mathcal{T}_h : T' \cap e \neq \emptyset\}$.

Proof. See [14]. □

We also need to introduce the Raviart-Thomas interpolation operator (see [7, 22]), $\Pi_h^k : [H^1(\Omega)]^{2 \times 2} \rightarrow H_h^\sigma$, which, for any given $\boldsymbol{\tau} \in [H^1(\Omega)]^{2 \times 2}$, is characterized by the following identities:

$$\int_e \Pi_h^k(\boldsymbol{\tau}) \mathbf{n} \cdot \mathbf{q} = \int_e \boldsymbol{\tau} \mathbf{n} \cdot \mathbf{q}, \quad \forall e \in E_h, \quad \forall \mathbf{q} \in [\mathcal{P}_k(e)]^2, \quad \text{when } k \geq 0, \quad (9)$$

and

$$\int_T \Pi_h^k(\boldsymbol{\tau}) : \boldsymbol{\rho} = \int_T \boldsymbol{\tau} : \boldsymbol{\rho}, \quad \forall T \in \mathcal{T}_h, \quad \forall \boldsymbol{\rho} \in [\mathcal{P}_{k-1}(T)]^{2 \times 2}, \quad \text{when } k \geq 1. \quad (10)$$

The operator Π_h^k satisfies the following approximation properties.

Lemma 3.2 *There exist constants $c_3, c_4, c_5 > 0$, independent of h , such that for all $T \in \mathcal{T}_h$*

$$\|\boldsymbol{\tau} - \Pi_h^k(\boldsymbol{\tau})\|_{[L^2(T)]^{2 \times 2}} \leq c_3 h_T^m |\boldsymbol{\tau}|_{[H^m(T)]^{2 \times 2}} \quad \forall \boldsymbol{\tau} \in [H^m(\Omega)]^{2 \times 2} \quad 1 \leq m \leq k+1 \quad (11)$$

and for all $\boldsymbol{\tau} \in [H^{m+1}(\Omega)]^{2 \times 2}$ with $\operatorname{div}(\boldsymbol{\tau}) \in [H^m(\Omega)]^2$,

$$\|\operatorname{div}(\boldsymbol{\tau} - \Pi_h^k(\boldsymbol{\tau}))\|_{[L^2(T)]^2} \leq c_4 h_T^m |\operatorname{div}(\boldsymbol{\tau})|_{[H^m(T)]^2} \quad 0 \leq m \leq k+1 \quad (12)$$

and

$$\|\boldsymbol{\tau} \mathbf{n} - \Pi_h^k(\boldsymbol{\tau}) \mathbf{n}\|_{[L^2(e)]^2} \leq c_5 h_e^{1/2} \|\boldsymbol{\tau}\|_{[H^1(T_e)]^{2 \times 2}} \quad \forall e \in E_h, \quad \forall \boldsymbol{\tau} \in [H^1(\Omega)]^{2 \times 2} \quad (13)$$

where $T_e \in \mathcal{T}_h$ contains e on its boundary.

Proof. See e.g. [7] or [22]. □

Moreover, the interpolation operator Π_h^k can also be defined as a bounded linear operator from the larger space $[H^s(\Omega)]^{2 \times 2} \cap H(\operatorname{div}; \Omega)$ into H_h^σ , for all $s \in (0, 1]$ (see, e.g. Theorem 3.16 in [19]). In this case, for any $\boldsymbol{\tau} \in [H^s(\Omega)]^{2 \times 2} \cap H(\operatorname{div}; \Omega)$, there holds the following interpolation error estimate

$$\|\boldsymbol{\tau} - \Pi_h^k(\boldsymbol{\tau})\|_{[L^2(T)]^{2 \times 2}} \leq C h_T^s \left\{ \|\boldsymbol{\tau}\|_{[H^s(T)]^{2 \times 2}} + \|\operatorname{div}(\boldsymbol{\tau})\|_{[L^2(T)]^2} \right\}, \quad \forall T \in \mathcal{T}_h.$$

Using (9) and (10), it is easy to show that

$$\operatorname{div}(\Pi_h^k(\boldsymbol{\tau})) = P_h^k(\operatorname{div}(\boldsymbol{\tau})), \quad \forall \boldsymbol{\tau} \in [H^s(\Omega)]^{2 \times 2} \cap H(\operatorname{div}; \Omega), \quad (14)$$

where $P_h^k : [L^2(\Omega)]^2 \rightarrow H_h^u$ is the L^2 -orthogonal projector. It is well known (see, e.g. [13]) that for each $\mathbf{v} \in [H^m(\Omega)]^2$, with $0 \leq m \leq k+1$, there holds

$$\|\mathbf{v} - P_h^k(\mathbf{v})\|_{[L^2(T)]^2} \leq C h_T^m |\mathbf{v}|_{[H^m(T)]^2}, \quad \forall T \in \mathcal{T}_h. \quad (15)$$

On the other hand, in order to prove the effectivity of the a posteriori error estimator, we use the localization technique introduced by Verfürth in [24]. Given $T \in \mathcal{T}_h$ and $e \in E(T)$, we let ψ_T and ψ_e be the usual triangle-bubble and edge-bubble functions (see equations (1.4) and (1.6) in [24], respectively), which satisfy:

1. $\psi_T \in \mathcal{P}_3(T)$, $\operatorname{supp}(\psi_T) \subseteq T$, $\psi_T = 0$ on ∂T and $0 \leq \psi_T \leq 1$ in T .
2. $\psi_e|_T \in \mathcal{P}_2(T)$, $\operatorname{supp}(\psi_e) \subseteq \omega_e := \cup\{T' \in \mathcal{T}_h : e \in E(T')\}$, $\psi_e = 0$ on $\partial T \setminus e$, and $0 \leq \psi_e \leq 1$ in ω_e .

We also recall from [23] that, given $k \in \mathbb{N} \cup \{0\}$, there exists a linear operator $L : \mathcal{C}(e) \rightarrow \mathcal{C}(T)$, $T \in \omega_e$, that satisfies $L(p) \in \mathcal{P}_k(T)$ and $L(p)|_e = p \quad \forall p \in \mathcal{P}_k(e)$. The corresponding vectorial version of L , that is, the component-wise application of L , is denoted by \mathbf{L} . Additional properties of ψ_T , ψ_e and L are collected in the following lemma.

Lemma 3.3 Given $k \in \mathbb{N} \cup \{0\}$, there exist positive constants c_6, c_7, c_8 , and c_9 , depending only on k and the shape regularity of the triangulations (minimum angle condition), such that for each $T \in \mathcal{T}_h$ and $e \in E(T)$, there hold

$$\|\psi_T q\|_{L^2(T)}^2 \leq \|q\|_{L^2(T)}^2 \leq c_6 \|\psi_T^{1/2} q\|_{L^2(T)}^2, \quad \forall q \in \mathcal{P}_k(T), \quad (16)$$

$$\|\psi_e L(p)\|_{L^2(T)}^2 \leq \|p\|_{L^2(e)}^2 \leq c_7 \|\psi_e^{1/2} p\|_{L^2(e)}^2, \quad \forall p \in \mathcal{P}_k(e), \quad (17)$$

and

$$c_8 h_e \|p\|_{L^2(e)}^2 \leq \|\psi_e^{1/2} L(p)\|_{L^2(T)}^2 \leq c_9 h_e \|p\|_{L^2(e)}^2, \quad \forall p \in \mathcal{P}_k(e). \quad (18)$$

Proof. See Lemma 4.1 in [23]. \square

The following inverse inequality will also be used.

Lemma 3.4 Let $l, m \in \mathbb{N} \cup \{0\}$ such that $l \leq m$. Then, there exists $c > 0$, depending only on k, l, m and the shape regularity of the triangulations, such that for each $T \in \mathcal{T}_h$ there holds

$$|q|_{H^m(T)} \leq c h_T^{l-m} |q|_{H^l(T)}, \quad \forall q \in \mathcal{P}_k(T).$$

Proof. See Theorem 3.2.6 in [13]. \square

3.2 Reliability

In order to derive a residual-based a posteriori error estimator, we first bound the error in terms of residuals.

Lemma 3.5 Let $(\boldsymbol{\sigma}, \mathbf{u}) \in \mathbf{H}_0$ and $(\boldsymbol{\sigma}_h, \mathbf{u}_h) \in \mathbf{H}_{0,h}$ be the unique solutions to problems (2) and (5), respectively. Then, there holds

$$\begin{aligned} C_{\text{ell}} \|(\boldsymbol{\sigma} - \boldsymbol{\sigma}_h, \mathbf{u} - \mathbf{u}_h)\|_{\mathbf{H}_0} &\leq \sup_{\substack{\boldsymbol{\tau} \in H(\mathbf{div}; \Omega) \\ \boldsymbol{\tau} \neq \mathbf{0}}} \frac{|R(\boldsymbol{\tau})|}{\|\boldsymbol{\tau}\|_{H(\mathbf{div}; \Omega)}} + \nu \|\mathbf{f} + \mathbf{div}(\boldsymbol{\sigma}_h) - \alpha \mathbf{u}_h\|_{[L^2(\Omega)]^2} \\ &\quad + \kappa_1 \|\nu \nabla \mathbf{u}_h - \boldsymbol{\sigma}_h^d\|_{[L^2(\Omega)]^{2 \times 2}}, \end{aligned} \quad (19)$$

where for all $\boldsymbol{\tau} \in H(\mathbf{div}; \Omega)$,

$$R(\boldsymbol{\tau}) := \nu \langle \boldsymbol{\tau} \mathbf{n}, \mathbf{g} \rangle_\Gamma - \int_{\Omega} \boldsymbol{\sigma}_h^d : \boldsymbol{\tau}^d - \nu \int_{\Omega} \mathbf{u}_h \cdot \mathbf{div}(\boldsymbol{\tau}) - \kappa_2 \int_{\Omega} (\mathbf{f} + \mathbf{div}(\boldsymbol{\sigma}_h) - \alpha \mathbf{u}_h) \cdot \mathbf{div}(\boldsymbol{\tau}).$$

Proof. Since $(\boldsymbol{\sigma} - \boldsymbol{\sigma}_h, \mathbf{u} - \mathbf{u}_h) \in \mathbf{H}_0$, we deduce, thanks to the ellipticity of the bilinear form $a(\cdot, \cdot)$, that

$$C_{\text{ell}} \|(\boldsymbol{\sigma} - \boldsymbol{\sigma}_h, \mathbf{u} - \mathbf{u}_h)\|_{\mathbf{H}_0} \leq \sup_{\substack{(\boldsymbol{\tau}, \mathbf{v}) \in \mathbf{H}_0 \\ (\boldsymbol{\tau}, \mathbf{v}) \neq (\mathbf{0}, \mathbf{0})}} \frac{a((\boldsymbol{\sigma} - \boldsymbol{\sigma}_h, \mathbf{u} - \mathbf{u}_h), (\boldsymbol{\tau}, \mathbf{v}))}{\|(\boldsymbol{\tau}, \mathbf{v})\|_{\mathbf{H}_0}}.$$

It is not difficult to verify that for any $(\boldsymbol{\tau}, \mathbf{v}) \in \mathbf{H}_0$

$$a((\boldsymbol{\sigma} - \boldsymbol{\sigma}_h, \mathbf{u} - \mathbf{u}_h), (\boldsymbol{\tau}, \mathbf{v})) = \nu \int_{\Omega} (\mathbf{f} + \operatorname{div}(\boldsymbol{\sigma}_h) - \alpha \mathbf{u}_h) \cdot \mathbf{v} - \kappa_1 \int_{\Omega} (\nu \nabla \mathbf{u}_h - \boldsymbol{\sigma}_h^d) : \nabla \mathbf{v} + R(\boldsymbol{\tau}).$$

Finally, inequality (19) is achieved after applying the Cauchy-Schwarz inequality and taking into account that

$$\sup_{\substack{\boldsymbol{\tau} \in H_0 \\ \boldsymbol{\tau} \neq \mathbf{0}}} \frac{|R(\boldsymbol{\tau})|}{\|\boldsymbol{\tau}\|_{H(\operatorname{div}; \Omega)}} \leq \sup_{\substack{\boldsymbol{\tau} \in H(\operatorname{div}; \Omega) \\ \boldsymbol{\tau} \neq \mathbf{0}}} \frac{|R(\boldsymbol{\tau})|}{\|\boldsymbol{\tau}\|_{H(\operatorname{div}; \Omega)}}.$$

We omit further details. \square

To bound the supremum on the right hand side of (19), we remark that since $R(\boldsymbol{\tau}_h) = 0$ for all $\boldsymbol{\tau}_h \in H_{0,h}^{\boldsymbol{\sigma}}$ and $R(\lambda \mathbf{I}) = 0$ for all $\lambda \in \mathbb{R}$, then $R(\boldsymbol{\tau}_h) = 0$ for all $\boldsymbol{\tau}_h \in H_h^{\boldsymbol{\sigma}}$ (a discrete subspace of $H(\operatorname{div}; \Omega)$). Thus we look for a suitable choice of $\boldsymbol{\tau}_h \in H_h^{\boldsymbol{\sigma}}$. Next, for each $\boldsymbol{\tau} \in H(\operatorname{div}; \Omega)$ we consider its Helmholtz decomposition

$$\boldsymbol{\tau} = \underline{\operatorname{curl}}(\boldsymbol{\chi}) + \nabla \mathbf{z},$$

where $\boldsymbol{\chi} \in [H^1(\Omega)]^2$ and $\mathbf{z} \in [H^2(\Omega)]^2$ satisfy $\Delta \mathbf{z} = \operatorname{div}(\boldsymbol{\tau})$ in Ω , and

$$\|\boldsymbol{\chi}\|_{[H^1(\Omega)]^2} + \|\mathbf{z}\|_{[H^2(\Omega)]^2} \leq C \|\boldsymbol{\tau}\|_{H(\operatorname{div}; \Omega)}.$$

Then, we let $\boldsymbol{\chi}_h := \mathbf{I}_h(\boldsymbol{\chi})$ and define

$$\boldsymbol{\tau}_h := \underline{\operatorname{curl}}(\boldsymbol{\chi}_h) + \Pi_h^k(\nabla \mathbf{z}) \in H_h^{\boldsymbol{\sigma}}. \quad (20)$$

We refer to (20) as a *discrete Helmholtz decomposition* of $\boldsymbol{\tau}_h$. Therefore, we can write

$$\boldsymbol{\tau} - \boldsymbol{\tau}_h = \underline{\operatorname{curl}}(\boldsymbol{\chi} - \boldsymbol{\chi}_h) + \nabla \mathbf{z} - \Pi_h^k(\nabla \mathbf{z}), \quad (21)$$

which, using (14) and that $\operatorname{div}(\nabla \mathbf{z}) = \Delta \mathbf{z} = \operatorname{div}(\boldsymbol{\tau})$ in Ω , yields

$$\operatorname{div}(\boldsymbol{\tau} - \boldsymbol{\tau}_h) = \operatorname{div}(\nabla \mathbf{z} - \Pi_h^k(\nabla \mathbf{z})) = (\mathbf{I} - P_h^k)(\operatorname{div}(\nabla \mathbf{z})) = (\mathbf{I} - P_h^k)(\operatorname{div}(\boldsymbol{\tau})). \quad (22)$$

Hence, taking into account (21) and (22) and integrating by parts, we can write

$$R(\boldsymbol{\tau}) = R(\boldsymbol{\tau} - \boldsymbol{\tau}_h) = R_1(\boldsymbol{\tau}) + R_2(\mathbf{z}) + R_3(\boldsymbol{\chi}),$$

where

$$\begin{aligned} R_1(\boldsymbol{\tau}) &:= -\kappa_2 \int_{\Omega} (\mathbf{f} + \operatorname{div}(\boldsymbol{\sigma}_h) - \alpha \mathbf{u}_h) \cdot (\mathbf{I} - P_h^k)(\operatorname{div}(\boldsymbol{\tau})), \\ R_2(\mathbf{z}) &:= \nu \langle (\nabla \mathbf{z} - \Pi_h^k(\nabla \mathbf{z})) \mathbf{n}, \mathbf{g} - \mathbf{u}_h \rangle_{\Gamma} - \int_{\Omega} (\boldsymbol{\sigma}_h^d - \nu \nabla \mathbf{u}_h) : (\nabla \mathbf{z} - \Pi_h^k(\nabla \mathbf{z})), \end{aligned}$$

and

$$R_3(\boldsymbol{\chi}) := \nu \langle (\underline{\operatorname{curl}}(\boldsymbol{\chi} - \boldsymbol{\chi}_h)) \mathbf{n}, \mathbf{g} - \mathbf{u}_h \rangle_{\Gamma} - \int_{\Omega} (\boldsymbol{\sigma}_h^d - \nu \nabla \mathbf{u}_h) : \underline{\operatorname{curl}}(\boldsymbol{\chi} - \boldsymbol{\chi}_h).$$

Our aim now is to obtain upper bounds for each one of the terms $R_1(\boldsymbol{\tau})$, $R_2(\mathbf{z})$ and $R_3(\boldsymbol{\chi})$.

Lemma 3.6 *There exists $C > 0$, independent of h , ν and α , such that for any $\boldsymbol{\tau} \in H(\mathbf{div}; \Omega)$ there holds*

$$|R_1(\boldsymbol{\tau})| \leq \kappa_2 \left(\sum_{T \in \mathcal{T}_h} \| \mathbf{f} + \mathbf{div}(\boldsymbol{\sigma}_h) - \alpha \mathbf{u}_h \|_{[L^2(T)]^2}^2 \right)^{1/2} \| \mathbf{div}(\boldsymbol{\tau}) \|_{[L^2(\Omega)]^2} .$$

Proof. The result follows from applying Cauchy-Schwarz inequality and (15) with $m = 0$. \square

Lemma 3.7 *There exists $C > 0$, independent of h , ν and α , such that*

$$|R_2(\mathbf{z})| \leq C \left(\sum_{e \in E_\Gamma} \nu^2 h_e \| \mathbf{g} - \mathbf{u}_h \|_{[L^2(e)]^2}^2 + \sum_{T \in \mathcal{T}_h} h_T^2 \| \boldsymbol{\sigma}_h^\mathbf{d} - \nu \nabla \mathbf{u}_h \|_{[L^2(T)]^{2 \times 2}}^2 \right)^{1/2} \| \boldsymbol{\tau} \|_{H(\mathbf{div}; \Omega)} .$$

Proof. Since $\nabla \mathbf{z} \in [H^1(\Omega)]^{2 \times 2}$, using Cauchy-Schwarz inequality and (13), we have

$$\begin{aligned} |\langle (\nabla \mathbf{z} - \Pi_h^k(\nabla \mathbf{z})) \mathbf{n}, \mathbf{g} - \mathbf{u}_h \rangle_\Gamma| &\leq \sum_{e \in E_\Gamma} \left| \int_e (\mathbf{g} - \mathbf{u}_h) \cdot (\nabla \mathbf{z} - \Pi_h^k(\nabla \mathbf{z})) \mathbf{n} \right| \\ &\leq \sum_{e \in E_\Gamma} \| (\nabla \mathbf{z} - \Pi_h^k(\nabla \mathbf{z})) \mathbf{n} \|_{[L^2(e)]^2} \| \mathbf{g} - \mathbf{u}_h \|_{[L^2(e)]^2} \leq c_5 \sum_{e \in E_\Gamma} h_e^{1/2} \| \nabla \mathbf{z} \|_{[H^1(T_e)]^{2 \times 2}} \| \mathbf{g} - \mathbf{u}_h \|_{[L^2(e)]^2} \\ &\leq c_5 \left(\sum_{e \in E_\Gamma} h_e \| \mathbf{g} - \mathbf{u}_h \|_{[L^2(e)]^2}^2 \right)^{1/2} \left(\sum_{e \in E_\Gamma} \| \nabla \mathbf{z} \|_{[H^1(T_e)]^{2 \times 2}}^2 \right)^{1/2} \\ &\leq c_5 \left(\sum_{e \in E_\Gamma} h_e \| \mathbf{g} - \mathbf{u}_h \|_{[L^2(e)]^2}^2 \right)^{1/2} \| \nabla \mathbf{z} \|_{[H^1(\Omega)]^{2 \times 2}} . \end{aligned}$$

Now, since $\| \nabla \mathbf{z} \|_{[H^1(\Omega)]^{2 \times 2}} \leq \| \mathbf{z} \|_{[H^2(\Omega)]^2} \leq C \| \boldsymbol{\tau} \|_{H(\mathbf{div}; \Omega)}$, we deduce

$$\nu |\langle (\nabla \mathbf{z} - \Pi_h^k(\nabla \mathbf{z})) \mathbf{n}, \mathbf{g} - \mathbf{u}_h \rangle_\Gamma| \leq C \left(\sum_{e \in E_\Gamma} h_e \nu^2 \| \mathbf{g} - \mathbf{u}_h \|_{[L^2(e)]^2}^2 \right)^{1/2} \| \boldsymbol{\tau} \|_{H(\mathbf{div}; \Omega)} .$$

Analogously, using Cauchy-Schwarz inequality and (11), we obtain

$$\left| \int_\Omega (\boldsymbol{\sigma}_h^\mathbf{d} - \nu \nabla \mathbf{u}_h) : (\nabla \mathbf{z} - \Pi_h^k(\nabla \mathbf{z})) \right| \leq C \left(\sum_{T \in \mathcal{T}_h} h_T^2 \| \boldsymbol{\sigma}_h^\mathbf{d} - \nu \nabla \mathbf{u}_h \|_{[L^2(\Omega)]^{2 \times 2}}^2 \right)^{1/2} \| \boldsymbol{\tau} \|_{H(\mathbf{div}; \Omega)} .$$

\square

Lemma 3.8 Assume $\mathbf{g} \in [H^1(\Gamma)]^2$. Then, there exists $C > 0$, independent of h , ν and α , such that

$$|R_3(\chi)| \leq C \left(\sum_{T \in \mathcal{T}_h} \|\boldsymbol{\sigma}_h^d - \nu \nabla \mathbf{u}_h\|_{[L^2(T)]^{2 \times 2}}^2 + \sum_{e \in E_\Gamma} h_e \nu^2 \left\| \frac{d\mathbf{g}}{dt} - \frac{d\mathbf{u}_h}{dt} \right\|_{[L^2(e)]^2}^2 \right)^{1/2} \|\boldsymbol{\tau}\|_{H(\mathbf{div}; \Omega)}.$$

Proof. We first remark that, for each $T \in \mathcal{T}_h$ we have

$$\|\underline{\mathbf{curl}}(\chi - \chi_h)\|_{[L^2(T)]^{2 \times 2}} = \|\nabla(\chi - \chi_h)\|_{[L^2(T)]^{2 \times 2}} \leq \|\chi - \chi_h\|_{[H^1(T)]^2},$$

which, using Lemma 3.1, implies

$$\|\underline{\mathbf{curl}}(\chi - \chi_h)\|_{[L^2(T)]^{2 \times 2}} \leq c_1 \|\chi\|_{[H^1(\omega(T))]^2}.$$

Then, applying Cauchy-Schwarz inequality, using that the number of triangles in $\omega(T)$ is bounded and $\|\chi\|_{[H^1(\Omega)]^2} \leq C \|\boldsymbol{\tau}\|_{H(\mathbf{div}; \Omega)}$, we deduce that

$$\left| \int_{\Omega} (\boldsymbol{\sigma}_h^d - \nu \nabla \mathbf{u}_h) : \underline{\mathbf{curl}}(\chi - \chi_h) \right| \leq C c_1 \left(\sum_{T \in \mathcal{T}_h} \|\boldsymbol{\sigma}_h^d - \nu \nabla \mathbf{u}_h\|_{[L^2(T)]^{2 \times 2}}^2 \right)^{1/2} \|\boldsymbol{\tau}\|_{H(\mathbf{div}; \Omega)}.$$

On the other hand, using that $\underline{\mathbf{curl}}(\chi - \chi_h) \mathbf{n} = -\frac{d}{dt}(\chi - \chi_h)$ on Γ , we arrive at

$$\nu \langle (\underline{\mathbf{curl}}(\chi - \chi_h)) \mathbf{n}, \mathbf{g} - \mathbf{u}_h \rangle_{\Gamma} = \nu \langle \chi - \chi_h, \frac{d}{dt}(\mathbf{g} - \mathbf{u}_h) \rangle_{\Gamma}.$$

Then, the proof follows applying Cauchy-Schwarz inequality and Lemma 3.1. \square

Motivated by these results, we define, for each $T \in \mathcal{T}_h$, the local error estimate η_T :

$$\begin{aligned} \eta_T^2 &:= \max\{\nu^2, \kappa_2^2\} \|\mathbf{f} + \mathbf{div}(\boldsymbol{\sigma}_h) - \alpha \mathbf{u}_h\|_{[L^2(T)]^2}^2 + \max\{\kappa_1^2, h_T^2, 1\} \|\boldsymbol{\sigma}_h^d - \nu \nabla \mathbf{u}_h\|_{[L^2(T)]^{2 \times 2}}^2 \\ &\quad + \sum_{e \in E_\Gamma \cap \partial T} \left(h_e \nu^2 \|\mathbf{g} - \mathbf{u}_h\|_{[L^2(e)]^2}^2 + \nu^2 h_e \left\| \frac{d\mathbf{g}}{dt} - \frac{d\mathbf{u}_h}{dt} \right\|_{[L^2(e)]^2}^2 \right). \end{aligned} \tag{23}$$

Finally, we present the following theorem, which establishes the reliability of the a posteriori error estimator $\eta := \left(\sum_{T \in \mathcal{T}_h} \eta_T^2 \right)^{1/2}$.

Theorem 3.1 Assume $\mathbf{g} \in [H^1(\Gamma)]^2$. Then, there exists $C > 0$, independent of h , ν and α , such that

$$\|(\boldsymbol{\sigma} - \boldsymbol{\sigma}_h, \mathbf{u} - \mathbf{u}_h)\|_{\mathbf{H}_0} \leq C C_{\text{ell}}^{-1} \eta. \tag{24}$$

Proof. It follows from Lemmas 3.5, 3.6, 3.7 and 3.8. \square

3.3 Efficiency

In this section we proceed to establish the local efficiency of the local a posteriori error estimate η_T (23). Since $\mathbf{f} = \alpha \mathbf{u} - \operatorname{div}(\boldsymbol{\sigma})$ in Ω and $\boldsymbol{\sigma}^d = \nu \nabla \mathbf{u}$ in Ω , we have that

$$\|\mathbf{f} + \operatorname{div}(\boldsymbol{\sigma}_h) - \alpha \mathbf{u}_h\|_{[L^2(T)]^2} \leq \alpha \|\mathbf{u} - \mathbf{u}_h\|_{[L^2(T)]^2} + \|\operatorname{div}(\boldsymbol{\sigma} - \boldsymbol{\sigma}_h)\|_{[L^2(T)]^2},$$

and

$$\|\nu \nabla \mathbf{u}_h - \boldsymbol{\sigma}_h^d\|_{[L^2(T)]^{2 \times 2}} \leq \nu |\mathbf{u} - \mathbf{u}_h|_{[H^1(T)]^2} + (1 + \sqrt{2}) \|\boldsymbol{\sigma} - \boldsymbol{\sigma}_h\|_{[L^2(T)]^{2 \times 2}}.$$

Now, in order to bound the boundary terms $h_e \|\mathbf{g} - \mathbf{u}_h\|_{[L^2(e)]^2}$, $e \in E_\Gamma$, we need to recall a discrete trace inequality. Indeed, as established in Theorem 3.10 in [1] (see also equation (2.4) in [3]), there exists $c > 0$, depending only on the shape regularity of the triangulations, such that for each $T \in \mathcal{T}_h$ and $e \in E(T)$, there holds

$$\|v\|_{L^2(e)}^2 \leq c \left\{ h_e^{-1} \|v\|_{L^2(T)}^2 + h_e |v|_{H^1(T)}^2 \right\}, \quad \forall v \in H^1(T). \quad (25)$$

Lemma 3.9 *There exists $C > 0$, independent of h , such that for each $e \in E_\Gamma$ there holds*

$$h_e \|\mathbf{g} - \mathbf{u}_h\|_{[L^2(e)]^2}^2 \leq C \left(\|\mathbf{u} - \mathbf{u}_h\|_{[L^2(T_e)]^2}^2 + h_{T_e}^2 |\mathbf{u} - \mathbf{u}_h|_{[H^1(T_e)]^2}^2 \right),$$

where T_e is the triangle having e as an edge.

Proof. It is a straightforward application of (25), taking into account that $\mathbf{u} = \mathbf{g}$ on Γ . \square

Lemma 3.10 *Assume $\mathbf{g} \in [H^1(\Gamma)]^2$ is component-piecewise polynomial on Γ . Then there exists $C > 0$, independent of h , such that for each $e \in E_\Gamma$ there holds*

$$h_e \left\| \frac{d\mathbf{g}}{dt} - \frac{d\mathbf{u}_h}{dt} \right\|_{[L^2(e)]^2}^2 \leq C |\mathbf{u} - \mathbf{u}_h|_{[H^1(T_e)]^2}^2, \quad (26)$$

where T_e is the triangle having e as an edge.

Proof. Let $e \in E_\Gamma$, and define $\boldsymbol{\chi}_e := \frac{d\mathbf{g}}{dt} - \frac{d\mathbf{u}_h}{dt}$ on e . Then, thanks to (17) and the extension operator $\mathbf{L} : [\mathcal{C}(e)]^2 \rightarrow [\mathcal{C}(T)]^2$, we obtain that

$$\|\boldsymbol{\chi}_e\|_{[L^2(e)]^2}^2 \leq c_7 \|\psi_e^{1/2} \boldsymbol{\chi}_e\|_{[L^2(e)]^2}^2 = c_7 \int_e \psi_e \boldsymbol{\chi}_e \cdot \left(\frac{d\mathbf{g}}{dt} - \frac{d\mathbf{u}_h}{dt} \right) = c_7 \int_{\partial T_e} \psi_e \mathbf{L}(\boldsymbol{\chi}_e) \cdot (\nabla \mathbf{u} - \nabla \mathbf{u}_h) \mathbf{t}.$$

Now, integrating by parts, we find that

$$\int_{\partial T_e} \psi_e \mathbf{L}(\boldsymbol{\chi}_e) \cdot (\nabla \mathbf{u} - \nabla \mathbf{u}_h) \mathbf{t} = \int_{T_e} \underline{\operatorname{curl}}(\psi_e \mathbf{L}(\boldsymbol{\chi}_e)) : (\nabla \mathbf{u} - \nabla \mathbf{u}_h).$$

Therefore, applying the Cauchy-Schwarz inequality and an inverse inequality, we have

$$\begin{aligned}
\|\boldsymbol{\chi}_e\|_{[L^2(e)]^2}^2 &\leq c_7 \|\underline{\text{curl}}(\psi_e \mathbf{L}(\boldsymbol{\chi}_e))\|_{[L^2(T_e)]^{2 \times 2}} \|\nabla \mathbf{u} - \nabla \mathbf{u}_h\|_{[L^2(T_e)]^{2 \times 2}} \\
&= c_7 |\psi_e \mathbf{L}(\boldsymbol{\chi}_e)|_{[H^1(T_e)]^2} |\mathbf{u} - \mathbf{u}_h|_{[H^1(T_e)]^2} \\
&\leq c_7 C h_e^{-1} \|\psi_e \mathbf{L}(\boldsymbol{\chi}_e)\|_{[L^2(T_e)]^2} |\mathbf{u} - \mathbf{u}_h|_{[H^1(T_e)]^2} \\
&\leq c_7 C h_e^{-1} \|\psi_e^{1/2} \mathbf{L}(\boldsymbol{\chi}_e)\|_{[L^2(T_e)]^2} |\mathbf{u} - \mathbf{u}_h|_{[H^1(T_e)]^2} \\
&\leq c_7 C c_9^{1/2} h_e^{-1} h_e^{1/2} \|\boldsymbol{\chi}_e\|_{[L^2(e)]^2} |\mathbf{u} - \mathbf{u}_h|_{[H^1(T_e)]^2},
\end{aligned}$$

and we end the proof. \square

In summary we have proved the next theorem, which establishes the local effectivity of the local a posteriori error estimator η_T .

Theorem 3.2 *Assume $\mathbf{g} \in [H^1(\Gamma)]^2$ is component-piecewise polynomial on Γ . Then, there exists $C = C(\nu, \kappa_1, \kappa_2, \alpha) > 0$, independent of h , such that for all $T \in \mathcal{T}_h$ we have*

$$\eta_T^2 \leq [C(\nu, \kappa_1, \kappa_2, \alpha)]^2 \left(\|\mathbf{u} - \mathbf{u}_h\|_{[H^1(T)]^2}^2 + \|\boldsymbol{\sigma} - \boldsymbol{\sigma}_h\|_{H(\mathbf{div}, T)}^2 \right).$$

Moreover, it is not difficult to see that $C(\nu, \kappa_1, \kappa_2, \alpha) = \mathcal{O}(\alpha)$. \square

4 A Ritz projection-based a posteriori error analysis

In this section, we consider the Ritz projection of the error with respect to the inner product of \mathbf{H}_0 , which is defined as the unique $(\bar{\boldsymbol{\sigma}}, \bar{\mathbf{u}}) \in \mathbf{H}_0$ satisfying

$$\langle (\bar{\boldsymbol{\sigma}}, \bar{\mathbf{u}}), (\boldsymbol{\tau}, \mathbf{v}) \rangle_{\mathbf{H}_0} = a((\boldsymbol{\sigma} - \boldsymbol{\sigma}_h, \mathbf{u} - \mathbf{u}_h), (\boldsymbol{\tau}, \mathbf{v})) \quad \forall (\boldsymbol{\tau}, \mathbf{v}) \in \mathbf{H}_0. \quad (27)$$

The existence and uniqueness of $(\bar{\boldsymbol{\sigma}}, \bar{\mathbf{u}})$ is guaranteed by the Lax-Milgram Lemma. Let us first obtain an upper bound for $\|(\bar{\boldsymbol{\sigma}}, \bar{\mathbf{u}})\|_{\mathbf{H}_0}$.

Lemma 4.1 *There exists a positive constant $C = C(\kappa_1, \kappa_2, \nu)$, independent of h , such that*

$$\|(\bar{\boldsymbol{\sigma}}, \bar{\mathbf{u}})\|_{\mathbf{H}_0} \leq C \left(\|\mathbf{f} + \mathbf{div}(\boldsymbol{\sigma}_h) - \alpha \mathbf{u}_h\|_{[L^2(\Omega)]^2} + \|\nu \nabla \mathbf{u}_h - \boldsymbol{\sigma}_h^d\|_{[L^2(\Omega)]^{2 \times 2}} + \nu \|\mathbf{u}_h - \mathbf{g}\|_{[H^{1/2}(\Gamma)]^2} \right).$$

Proof. Using the fact that $(\boldsymbol{\sigma}, \mathbf{u})$ is the solution of (2) and the definition of the bilinear form $a(\cdot, \cdot)$, we notice that problem (27) is equivalent to

$$\begin{aligned}
\langle \bar{\boldsymbol{\sigma}}, \boldsymbol{\tau} \rangle_{\mathbf{H}_0} &= G_1(\boldsymbol{\tau}) \quad \forall \boldsymbol{\tau} \in \mathbf{H}_0, \\
\langle \bar{\mathbf{u}}, \mathbf{v} \rangle_{[H^1(\Omega)]^2} &= G_2(\mathbf{v}) \quad \forall \mathbf{v} \in [H^1(\Omega)]^2,
\end{aligned}$$

where G_1 and G_2 are linear and bounded functionals defined, for any $\boldsymbol{\tau} \in H(\mathbf{div}; \Omega)$ and $\mathbf{v} \in [H^1(\Omega)]^2$, respectively, by

$$G_1(\boldsymbol{\tau}) := -\kappa_2 \int_{\Omega} (\mathbf{f} + \mathbf{div}(\boldsymbol{\sigma}_h) - \alpha \mathbf{u}_h) \cdot \mathbf{div}(\boldsymbol{\tau}) + \int_{\Omega} (\nu \nabla \mathbf{u}_h - \boldsymbol{\sigma}_h^d) : \boldsymbol{\tau} - \nu \langle \mathbf{u}_h - \mathbf{g}, \boldsymbol{\tau} \mathbf{n} \rangle_{\Gamma},$$

and

$$G_2(\mathbf{v}) := -\kappa_1 \int_{\Omega} (\nu \nabla \mathbf{u}_h - \boldsymbol{\sigma}_h^d) : (\nabla \mathbf{v}) + \nu \int_{\Omega} (\mathbf{f} + \mathbf{div}(\boldsymbol{\sigma}_h) - \alpha \mathbf{u}_h) \cdot \mathbf{v}.$$

Then, applying the Cauchy-Schwarz inequality, we have

$$\|\bar{\boldsymbol{\sigma}}\|_{H_0} \leq \kappa_2 \|\mathbf{f} + \mathbf{div}(\boldsymbol{\sigma}_h) - \alpha \mathbf{u}_h\|_{[L^2(\Omega)]^2} + \|\nu \nabla \mathbf{u}_h - \boldsymbol{\sigma}_h^d\|_{[L^2(\Omega)]^{2 \times 2}} + \nu \|\mathbf{u}_h - \mathbf{g}\|_{[H^{1/2}(\Gamma)]^2},$$

and

$$\|\bar{\mathbf{u}}\|_{[H_1(\Omega)]^2} \leq \nu \|\mathbf{f} + \mathbf{div}(\boldsymbol{\sigma}_h) - \alpha \mathbf{u}_h\|_{[L^2(\Omega)]^2} + \kappa_1 \|\nu \nabla \mathbf{u}_h - \boldsymbol{\sigma}_h^d\|_{[L^2(\Omega)]^{2 \times 2}}.$$

This completes the proof of this Lemma. \square

Motivated by the previous result, we define the a posteriori error estimator θ as follows:

$$\theta^2 := \sum_{T \in \mathcal{T}_h} \left(\|\mathbf{f} + \mathbf{div}(\boldsymbol{\sigma}_h) - \alpha \mathbf{u}_h\|_{[L^2(T)]^2}^2 + \|\nu \nabla \mathbf{u}_h - \boldsymbol{\sigma}_h^d\|_{[L^2(T)]^{2 \times 2}}^2 \right) + \nu \|\mathbf{u}_h - \mathbf{g}\|_{[H^{1/2}(\Gamma)]^2}^2,$$

where \mathcal{T}_h is some triangulation of the domain Ω . In the next theorem, we establish the equivalence between the total error and the estimator θ .

Theorem 4.1 *Let $(\boldsymbol{\sigma}, \mathbf{u}) \in \mathbf{H}_0$ and $(\boldsymbol{\sigma}_h, \mathbf{u}_h) \in \mathbf{H}_{0,h}$ be the unique solutions to problems (2) and (5), respectively. Then, there exist positive constants C_{eff} , C_{rel} , independent of h , such that*

$$C_{\text{eff}} \theta \leq \|(\boldsymbol{\sigma} - \boldsymbol{\sigma}_h, \mathbf{u} - \mathbf{u}_h)\|_{\mathbf{H}_0} \leq C_{\text{rel}} \theta.$$

Proof. Applying the coercivity of the bilinear form $a(\cdot, \cdot)$ to the error $(\boldsymbol{\sigma} - \boldsymbol{\sigma}_h, \mathbf{u} - \mathbf{u}_h) \in \mathbf{H}_0$ and using the definition of the Ritz projection (27), we deduce that

$$\begin{aligned} \|(\boldsymbol{\sigma} - \boldsymbol{\sigma}_h, \mathbf{u} - \mathbf{u}_h)\|_{\mathbf{H}_0} &\leq C_{\text{ell}}^{-1} \frac{a((\boldsymbol{\sigma} - \boldsymbol{\sigma}_h, \mathbf{u} - \mathbf{u}_h), (\boldsymbol{\sigma} - \boldsymbol{\sigma}_h, \mathbf{u} - \mathbf{u}_h))}{\|(\boldsymbol{\sigma} - \boldsymbol{\sigma}_h, \mathbf{u} - \mathbf{u}_h)\|_{\mathbf{H}_0}} \\ &\leq C_{\text{ell}}^{-1} \sup_{\substack{(\boldsymbol{\tau}, \mathbf{v}) \in \mathbf{H}_0 \\ (\boldsymbol{\tau}, \mathbf{v}) \neq (\mathbf{0}, \mathbf{0})}} \frac{a((\boldsymbol{\sigma} - \boldsymbol{\sigma}_h, \mathbf{u} - \mathbf{u}_h), (\boldsymbol{\tau}, \mathbf{v}))}{\|(\boldsymbol{\tau}, \mathbf{v})\|_{\mathbf{H}_0}} \\ &= C_{\text{ell}}^{-1} \sup_{\substack{(\boldsymbol{\tau}, \mathbf{v}) \in \mathbf{H}_0 \\ (\boldsymbol{\tau}, \mathbf{v}) \neq (\mathbf{0}, \mathbf{0})}} \frac{\langle (\bar{\boldsymbol{\sigma}}, \bar{\mathbf{u}}), (\boldsymbol{\tau}, \mathbf{v}) \rangle}{\|(\boldsymbol{\tau}, \mathbf{v})\|_{\mathbf{H}_0}} = C_{\text{ell}}^{-1} \|(\bar{\boldsymbol{\sigma}}, \bar{\mathbf{u}})\|_{\mathbf{H}_0}, \end{aligned}$$

which yields, using Lemma 4.1 and the definition of θ , that the a posteriori error estimator θ is reliable.

On the other hand, for the proof of the efficiency of θ , we take into account the relations (25), (25), and a trace theorem to derive

$$\|\mathbf{u}_h - \mathbf{g}\|_{[H^{1/2}(\Gamma)]^2} \leq C \|\mathbf{u}_h - \mathbf{u}\|_{[H^1(\Omega)]^2}.$$

□

In the rest of this section, we assume more regularity on \mathbf{g} in order to define a local estimator. More precisely, we assume that $\mathbf{g} \in [H^1(\Gamma)]^2$ so that we can define

$$\hat{\theta}^2 := \sum_{T \in \mathcal{T}_h} \left(\|\mathbf{f} + \operatorname{div}(\boldsymbol{\sigma}_h) - \alpha \mathbf{u}_h\|_{[L^2(T)]^2}^2 + \|\nu \nabla \mathbf{u}_h - \boldsymbol{\sigma}_h^d\|_{[L^2(T)]^{2 \times 2}}^2 + \nu \sum_{e \in E(T) \cap E_\Gamma} \|\mathbf{g} - \mathbf{u}_h\|_{[H^1(e)]^2}^2 \right).$$

Theorem 4.2 Assume that $\mathbf{g} \in [H^1(\Gamma)]^2$. Then, there exists a constant $C_{\text{rel}} > 0$, independent of h , such that

$$\|(\boldsymbol{\sigma} - \boldsymbol{\sigma}_h, \mathbf{u} - \mathbf{u}_h)\|_{\mathbf{H}_0} \leq C_{\text{rel}} \hat{\theta}.$$

Proof. Using that $[H^{1/2}(\Gamma)]^2$ is the interpolation space of index 1/2 between $[L^2(\Gamma)]^2$ and $[H^1(\Gamma)]^2$, we have that

$$\|\mathbf{g} - \mathbf{u}_h\|_{[H^{1/2}(\Gamma)]^2}^2 \leq C \|\mathbf{g} - \mathbf{u}_h\|_{[L^2(\Gamma)]^2} \|\mathbf{g} - \mathbf{u}_h\|_{[H^1(\Gamma)]^2} \leq C \sum_{e \in E_\Gamma} \|\mathbf{g} - \mathbf{u}_h\|_{[H^1(e)]^2}^2.$$

Then, the result follows from Theorem 4.1, the previous inequality and the definition of $\hat{\theta}$. □

Alternatively, we can follow [6] and let $\bar{\mathbf{u}}_h$ be the unique continuous piecewise-linear function on \mathcal{T}_h such that $\bar{\mathbf{u}}_h(\mathbf{x}) = \mathbf{u}_h(\mathbf{x})$ for all node \mathbf{x} of \mathcal{T}_h in Ω and $\bar{\mathbf{u}}_h(\mathbf{x}) = \mathbf{g}(\mathbf{x})$ for all node \mathbf{x} of \mathcal{T}_h on Γ . Then, by virtue of Theorem 1 in [12], if $\mathbf{g} \in [H^1(\Gamma)]^2$, then there exists a constant $C > 0$, independent of h , such that

$$\|\mathbf{g} - \bar{\mathbf{u}}_h\|_{[H^{1/2}(\Gamma)]^2}^2 \leq C \log(1 + \kappa) \sum_{e \in E_\Gamma} h_e \left\| \frac{d\mathbf{g}}{dt} - \frac{d\bar{\mathbf{u}}_h}{dt} \right\|_{[L^2(e)]^2}^2, \quad (28)$$

where $\kappa := \max \left\{ \frac{h_{e_i}}{h_{e_j}} : \text{such that } e_i, e_j \text{ are consecutive edges on } \Gamma \right\}$. Proceeding analogously to Section 3 (see (26)), we also have the following lemma.

Lemma 4.2 Assume that each component of \mathbf{g} is a piecewise polynomial on Γ . Then, there exists a constant $C > 0$, independent of h , such that

$$h_e \left\| \frac{d\mathbf{g}}{dt} - \frac{d\bar{\mathbf{u}}_h}{dt} \right\|_{[L^2(e)]^2}^2 \leq C \|\mathbf{u} - \bar{\mathbf{u}}_h\|_{[H^1(T_e)]^2}^2, \quad \forall e \in E_\Gamma,$$

where T_e is the triangle that has e as an edge.

Then, we may define the a posteriori error estimate $\bar{\theta} := \left(\sum_{T \in \mathcal{T}_h} \bar{\theta}_T^2 \right)^{1/2}$, where

$$\begin{aligned} \bar{\theta}_T^2 &:= \| \mathbf{f} + \operatorname{div}(\boldsymbol{\sigma}_h) - \alpha \mathbf{u}_h \|_{[L^2(T)]^2}^2 + \| \nu \nabla \bar{\mathbf{u}}_h - \boldsymbol{\sigma}_h^d \|_{[L^2(T)]^{2 \times 2}}^2 + \| \mathbf{u}_h - \bar{\mathbf{u}}_h \|_{[L^2(T)]^2}^2 \\ &+ \log(1 + \kappa) \sum_{e \in E(T) \cap E_\Gamma} h_e \left\| \frac{d\mathbf{g}}{dt_T} - \frac{d\bar{\mathbf{u}}_h}{dt_T} \right\|_{[L^2(e)]^2}^2. \end{aligned} \quad (29)$$

Theorem 4.3 Assume $\mathbf{g} \in [H^1(\Gamma)]^2$. Then, there exists a constant $C_{\text{rel}} > 0$, independent of h , such that

$$\| (\boldsymbol{\sigma} - \boldsymbol{\sigma}_h, \mathbf{u} - \mathbf{u}_h) \|_{\mathbf{H}_0} \leq C_{\text{rel}} \bar{\theta}.$$

If, moreover, each component of \mathbf{g} is a piecewise polynomial on Γ , then there exists a positive constant, C_{eff} , independent of h , such that

$$C_{\text{eff}} \bar{\theta}_T^2 \leq \| (\boldsymbol{\sigma} - \boldsymbol{\sigma}_h, \mathbf{u} - \mathbf{u}_h) \|_{\mathbf{H}(T)}^2 + \nu \chi(T) \| \mathbf{u}_h - \bar{\mathbf{u}}_h \|_{[H^1(T)]^2}^2, \quad \forall T \in \mathcal{T}_h,$$

where $\| (\boldsymbol{\tau}, \mathbf{v}) \|_{\mathbf{H}(T)}^2 := \| \boldsymbol{\tau} \|_{H(\operatorname{div}; T)}^2 + \| \mathbf{v} \|_{[H^1(T)]^2}^2$ and $\chi(T)$ is equal to 1 if $\partial T \cap \Gamma \neq \emptyset$ and is equal to 0 otherwise.

Proof. We proceed as in the proof of Lemma 4.1 but, before integrating by parts in G_1 , we write

$$\int_{\Omega} \mathbf{u}_h \cdot \operatorname{div}(\boldsymbol{\tau}) = \int_{\Omega} (\mathbf{u}_h - \bar{\mathbf{u}}_h) \cdot \operatorname{div}(\boldsymbol{\tau}) + \int_{\Omega} \bar{\mathbf{u}}_h \cdot \operatorname{div}(\boldsymbol{\tau}).$$

Next, we integrate by parts in the last term on the right-hand side and obtain that

$$\begin{aligned} \| (\bar{\boldsymbol{\sigma}}, \bar{\mathbf{u}}) \|_{\mathbf{H}_0} &\leq C \left(\| \mathbf{f} + \operatorname{div}(\boldsymbol{\sigma}_h) - \alpha \mathbf{u}_h \|_{[L^2(\Omega)]^2}^2 + \| \nu \nabla \bar{\mathbf{u}}_h - \boldsymbol{\sigma}_h^d \|_{[L^2(\Omega)]^{2 \times 2}}^2 + \nu \| \mathbf{u}_h - \bar{\mathbf{u}}_h \|_{[L^2(\Omega)]^2}^2 \right. \\ &\quad \left. + \nu \| \mathbf{g} - \bar{\mathbf{u}}_h \|_{[H^{1/2}(\Gamma)]^2}^2 \right)^{1/2}, \end{aligned}$$

where $C > 0$ is a constant independent of h . Then, the reliability follows from Theorem 4.1, the previous bound, (28) and the definition of $\bar{\theta}$.

On the other hand, let $T \in \mathcal{T}_h$. If $T \subset \Omega$, then $\mathbf{u}_h = \bar{\mathbf{u}}_h$ in T and we can substitute $\nabla \bar{\mathbf{u}}_h$ by $\nabla \mathbf{u}_h$ in the second term on the right-hand side of (29). Moreover, the two last terms in (29) vanish in this case and the effectivity follows proceeding as in the proof of Theorem 4.1. When $\partial T \cap \Gamma \neq \emptyset$, the result follows applying Lemma 4.2 and using the triangle inequality in the second term on the right-hand side of (29). \square

As a consequence, we have obtained a reliable and fully local a posteriori error estimate, $\bar{\theta}$, that is locally efficient except in those elements with a node or a side on the boundary Γ .

Finally, we remark that slight modifications of the a posteriori error analyses developed in Sections 3 and 4, allow us to establish the corresponding a posteriori error estimators for the other formulations analysed in [5]. We omit further details, for the sake of simplicity.

5 Numerical results

We begin this section by remarking that, for implementation purposes, it is very hard to find a suitable basis of $H_{0,h}^\sigma$ due to the null media condition required by their elements. We circumvent this difficulty by imposing this requirement through a Lagrange multiplier. More precisely, we solve the following auxiliary discrete scheme: Find $(\boldsymbol{\sigma}_h, \mathbf{u}_h, \varphi_h) \in \mathbf{H}_h := H_h^\sigma \times H_h^u \times \mathbb{R}$ such that

$$\begin{aligned} a((\boldsymbol{\sigma}_h, \mathbf{u}_h), (\boldsymbol{\tau}_h, \mathbf{v}_h)) + \varphi_h \int_\Omega \text{tr}(\boldsymbol{\tau}_h) &= F(\boldsymbol{\tau}_h, \mathbf{v}_h), \\ \psi_h \int_\Omega \text{tr}(\boldsymbol{\sigma}_h) &= 0, \end{aligned} \tag{30}$$

for all $(\boldsymbol{\tau}_h, \mathbf{v}_h, \psi_h) \in \mathbf{H}_h$. The next theorem establishes the equivalence between the variational problems (5) and (30).

Theorem 5.1

- i) Let $(\boldsymbol{\sigma}_h, \mathbf{u}_h) \in \mathbf{H}_{0,h}$ be a solution of (5). Then $(\boldsymbol{\sigma}_h, \mathbf{u}_h, 0)$ is a solution of (30).
- ii) Let $(\boldsymbol{\sigma}_h, \mathbf{u}_h, \varphi_h) \in \mathbf{H}_h$ be a solution of (30). Then $\varphi_h = 0$ and $(\boldsymbol{\sigma}_h, \mathbf{u}_h)$ is a solution of (5).

Proof. We adapt the proof of Theorem 4.3 in [15]. We first observe, according to the definition of $a(\cdot, \cdot)$, that for each $(\boldsymbol{\tau}, \mathbf{v}) \in H(\text{div}; \Omega) \times [H^1(\Omega)]^2$ there holds

$$a((\boldsymbol{\tau}, \mathbf{v}), (\mathbf{I}, 0)) = 0 \quad \forall (\boldsymbol{\tau}, \mathbf{v}) \in H(\text{div}; \Omega) \times [H^1(\Omega)]^2. \tag{31}$$

Now, let $(\boldsymbol{\sigma}_h, \mathbf{u}_h) \in \mathbf{H}_{0,h}$ be the solution of (5), and let $(\boldsymbol{\tau}_h, \mathbf{v}_h) \in \mathbf{H}_h^\sigma \times H_h^u$. We write $\boldsymbol{\tau}_h = \boldsymbol{\tau}_{0,h} + d_h \mathbf{I}$, with $\boldsymbol{\tau}_{0,h} \in \mathbf{H}_{0,h}^\sigma$ and $d_h \in \mathbb{R}$, and observe that $(\boldsymbol{\tau}_{0,h}, \mathbf{v}_h) \in \mathbf{H}_{0,h}$, whence the definition of F , (5) and (31) yield

$$F(\boldsymbol{\tau}_h, \mathbf{v}_h) = F(\boldsymbol{\tau}_{0,h}, \mathbf{v}_h) = a((\boldsymbol{\sigma}_h, \mathbf{u}_h), (\boldsymbol{\tau}_{0,h}, \mathbf{v}_h)) = a((\boldsymbol{\sigma}_h, \mathbf{u}_h), (\boldsymbol{\tau}_h, \mathbf{v}_h)).$$

This identity and the fact that $\boldsymbol{\sigma}_h$ clearly satisfies the second equation of (30), show that $(\boldsymbol{\sigma}_h, \mathbf{u}_h, 0)$ is indeed a solution of (30).

Conversely, let $(\boldsymbol{\sigma}_h, \mathbf{u}_h, \varphi_h) \in \mathbf{H}_h$ be a solution of (30). Then taking $(\boldsymbol{\tau}_h, \mathbf{v}_h) = (\mathbf{I}, 0)$ in the first equation of (30) and using the definition of F and (31), we find that $\varphi_h = 0$, whence $(\boldsymbol{\sigma}_h, \mathbf{u}_h)$ becomes the solution of (5). \square

We now specify the data of the three examples to be presented here. We take Ω as either the square $[-1, 1]^2$ (for Example 1), the square $[0, 1]^2$ (for Example 3) or the circular section $\Omega := \{(x_1, x_2) \in \mathbb{R}^2 : x_1^2 + x_2^2 < 1\} \setminus ([0, 1] \times [-1, 0])$ (for Example 2). In all examples, the data \mathbf{f} and \mathbf{g} are chosen so that the exact solutions \mathbf{u} and p of (1) are the ones shown in

Table 1, where $s = \sqrt{(x_1 - 2)^2 + (x_2 - 2)^2}$. We remind that in all cases, $\operatorname{div}(\mathbf{u}) = 0$ in Ω and $\boldsymbol{\sigma} = \nu \nabla \mathbf{u} - p \mathbf{I}$ in Ω . We emphasize that the solution (\mathbf{u}, p) of Example 1 is smooth. The solution $\mathbf{u} \in [H^1(\Omega)]^2$ for Example 3 has an inner layer around the line $x_2 = 0.5 - x_1$, while the exact pressure p in Example 2 lives in $H^{1+2/3}(\Omega)$, since their derivatives are singular at $(0, 0)$. This implies that $\operatorname{div}(\boldsymbol{\sigma}) \in [H^{2/3}(\Omega)]^2$ only, which, according to Theorem 2.1, yields $2/3$ as the expected rate of convergence for the uniform refinement.

In what follows, DOF stands for the total number of degrees of freedom (unknowns) of (30), that is, $DOF = 2 \times (\text{Number of vertices of } \mathcal{T}_h) + 2 \times (\text{Number of edges of } \mathcal{T}_h) + 1$, which leads asymptotically to 4 unknowns per triangle, which reflects the low computational cost, almost the same than the required by considering the \mathbb{P}_1 -iso \mathbb{P}_1 elements for the standard velocity-pressure formulation, whose degrees of freedom are asymptotically 4.5 (unknowns) per triangle. In addition, by setting $p_h := -\frac{1}{2} \operatorname{tr}(\boldsymbol{\sigma}_h)$, we obtain a reasonable piecewise-linear approximation of the pressure $p = -\frac{1}{2} \operatorname{tr}(\boldsymbol{\sigma})$. Hereafter, the individual and total errors are denoted as follows

$$\begin{aligned} \mathbf{e}(\mathbf{u}) &:= \|\mathbf{u} - \mathbf{u}_h\|_{[H^1(\Omega)]^2}, \quad \mathbf{e}(\boldsymbol{\sigma}) := \|\boldsymbol{\sigma} - \boldsymbol{\sigma}_h\|_{H(\operatorname{div}, \Omega)}, \quad \mathbf{e} := \left([\mathbf{e}(\mathbf{u})]^2 + [\mathbf{e}(\boldsymbol{\sigma})]^2 \right)^{1/2}, \\ \mathbf{e}_0(p) &:= \left\| p + \frac{1}{2} \operatorname{tr}(\boldsymbol{\sigma}_h) \right\|_{L^2(\Omega)}, \quad \mathbf{e}_0(\boldsymbol{\sigma}^d) := \|\boldsymbol{\sigma}^d - \boldsymbol{\sigma}_h^d\|_{[L^2(\Omega)]^{2 \times 2}}, \\ \text{and} \quad \mathbf{e}_0(\mathbf{u}) &:= \|\mathbf{u} - \mathbf{u}_h\|_{[L^2(\Omega)]^2}, \end{aligned}$$

where $(\boldsymbol{\sigma}, \mathbf{u}) \in H_0 \times [H^1(\Omega)]^2$ and $(\boldsymbol{\sigma}_h, \mathbf{u}_h) \in H_{0,h}^\sigma \times H_h^u$ are the unique solutions of the continuous and discrete formulations, respectively. In addition, if \mathbf{e} and $\tilde{\mathbf{e}}$ stand for the errors at two consecutive triangulations with N and \tilde{N} degrees of freedom, respectively, then the experimental rate of convergence is given by $r := -2 \frac{\log(\mathbf{e}/\tilde{\mathbf{e}})}{\log(N/\tilde{N})}$. The definitions of $r(\mathbf{u})$, $r(\boldsymbol{\sigma})$, $r_0(\boldsymbol{\sigma}^d)$, $r_0(\mathbf{u})$ and $r_0(p)$ are defined analogously.

On the other hand, the adaptive algorithm used in the mesh refinement process based on an estimator ζ_T (which can be η_T or $\bar{\theta}_T$) is the following (see [24]):

1. Start with a coarse mesh \mathcal{T}_h .
2. Solve the Galerkin scheme (30) for the current mesh \mathcal{T}_h .
3. Compute ζ_T for each triangle $T \in \mathcal{T}_h$.
4. Consider stopping criterion and decide to finish or go to the next step.
5. Use *Red-blue-green* procedure to refine each element $T' \in \mathcal{T}_h$ such that

$$\zeta_{T'} \geq \frac{1}{2} \max\{\zeta_T : T \in \mathcal{T}_h\}.$$

EXAMPLE	\mathbf{u}	p
1	$\begin{pmatrix} -e^{x_1}(x_2 \cos(x_2) + \sin(x_2)) \\ e^{x_1}x_2 \sin(x_2) \end{pmatrix}$	$2e^{x_1} \sin(x_2)$
2	$\frac{1}{8\pi\nu} \left\{ -\ln(s) \begin{pmatrix} 1 \\ 0 \end{pmatrix} + \frac{1}{s^2} \begin{pmatrix} (x_1 - 2)^2 \\ (x_1 - 2)(x_2 - 1) \end{pmatrix} \right\}$	$r^{2/3} \sin\left(\frac{2}{3}\theta\right) - \frac{3}{2\pi}$
3	$-\sqrt{\alpha}e^{-\sqrt{\alpha}(0.5-x_1-x_2)^2} \begin{pmatrix} 1 \\ -1 \end{pmatrix}$	$2e^{2x_1-1} \sin(2x_2 - 1)$

Table 1: Summary of data for the three examples.

6. Define the resulting mesh as the new \mathcal{T}_h and go to step 2.

In addition, with the aim of showing the robustness of the augmented method with respect to the parameters α and ν , and thus for the parameters (κ_1, κ_2) , included in the definition of the bilinear form $a(\cdot, \cdot)$ (cf. (3)), as well as the linear functional $F(\cdot)$ (cf. (4)), we consider different values for α and ν , and we set $\kappa_1 = \nu$ and $\kappa_2 = \nu/\alpha$ in agreement with the feasible choices described in Section 2. From now on, we assume that the viscosity $\nu = 1$ for Examples 1 and 2, and $\nu = 0.5$ for Example 3.

In Figures 1-6 we exhibit the total error vs degrees of freedom and the effectivity index vs DOF , for adaptive and uniform refinements, for Example 1, with different values of α . Hereafter uniform refinement means that, given a uniform initial triangulation, each subsequent mesh is obtained from the previous one by dividing each triangle into the four ones arising when connecting the midpoints of its sides. We note that in all cases the effectivity index for both estimators is almost constant. As parameter α grows, it is necessary to use finest meshes in order to attain optimal convergence and almost constant effectivity indices. We observe, as expected, that for α large, a small enough mesh size is needed to get optimal convergence.

In Tables 2 through 15 we provide the individual and total errors, the experimental rates of convergence, and the effectivity indices for adaptive refinements as applied to Examples 2 and 3, using both estimators with different values of the parameter α . We observe from these tables that the errors of the adaptive procedure decrease at least than those obtained by the uniform one, which is confirmed by the experimental rates of convergence.

This fact can also be seen in Figures 8-11, where we display the total error e versus the degrees of freedom DOF for uniform and adaptive refinements, for Example 2, for different values of α . In addition, in Figure 7 we show the behavior of individual errors vs DOF ,

$(\alpha = 10^2)$ which is in agreement with the theory. It is shown there that the global error \mathbf{e} is dominated by the error in pseudostress $\mathbf{e}(\boldsymbol{\sigma})$.

Due to the singularity of the velocity \mathbf{u} in this example, we notice that $r(\mathbf{e})$ approaches to $2/3$ for the uniform refinement, as expected, and the adaptives methods are able to recover, at least numerically, the corresponding rate of convergence $\mathcal{O}(h)$ for the total error. Similarly to the smooth case, when α is large, we need finest adaptive meshes to recover the rates of convergence. This phenomena can be explained due to two facts. The first one is that in these cases the error in the pseudostress $\mathbf{e}(\boldsymbol{\sigma})$ is large enough such that it dominates the behavior of total error \mathbf{e} , and thus obtaining the theoretical rate of convergence. The second cause, but not less important, is that the regularity effect of α is a global phenomena and not a local one. Furthermore, the effectivity indices remain again bounded from above and below, which confirms the reliability and effectivity of η and $\bar{\theta}$ for the adaptive algorithms.

In Figures 12 and 13 we display the total error \mathbf{e} versus the degrees of freedom DOF , for Example 3, considering both refinements. As expected we notice that for this case, the error of the adaptive refinements decrease much faster than the uniform one when the parameter α is increasing. Finally, we show in Figures 14-17 the adapted meshes obtained in Example 2 and 3 by our estimators. We point out that both two a posteriori error estimators are able to detect and refine surrounding the singularity of the velocity in Example 2 (see Figures 14-15) as well as the inner layer for Example 3 (see Figures 16-17).

Acknowledgements

The first author is supported by Dirección de Investigación, Universidad Católica de la Santísima Concepción. The second author acknowledges partial support by FONDECYT Grant 1130158; BASAL project CMM, U. de Chile and Centro de Investigación en Ingeniería Matemática (CI²MA), Universidad de Concepción; and CONICYT project Anillo ACT1118 (ANANUM). Third author is partially supported by FONDECYT Grant 1120560. The fourth author is supported by MICINN through Grant MTM2010-21135-C02-01 and by Xunta de Galicia through INCITE09 105339PR.

In addition, the authors want to express their gratitude to Professor José Manuel Cascón, from Universidad de Salamanca (Spain), for his valuable opinion and suggestions on the discussions of the numerical results included in the present work.

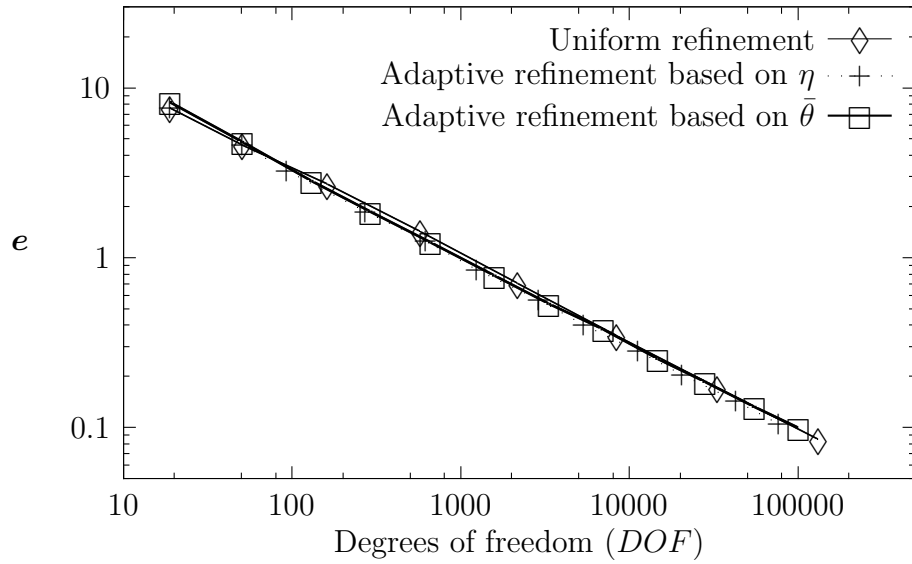


Figure 1: Total error e vs DOF for uniform and adaptive refinements (Ex. 1, $\alpha = 1$).

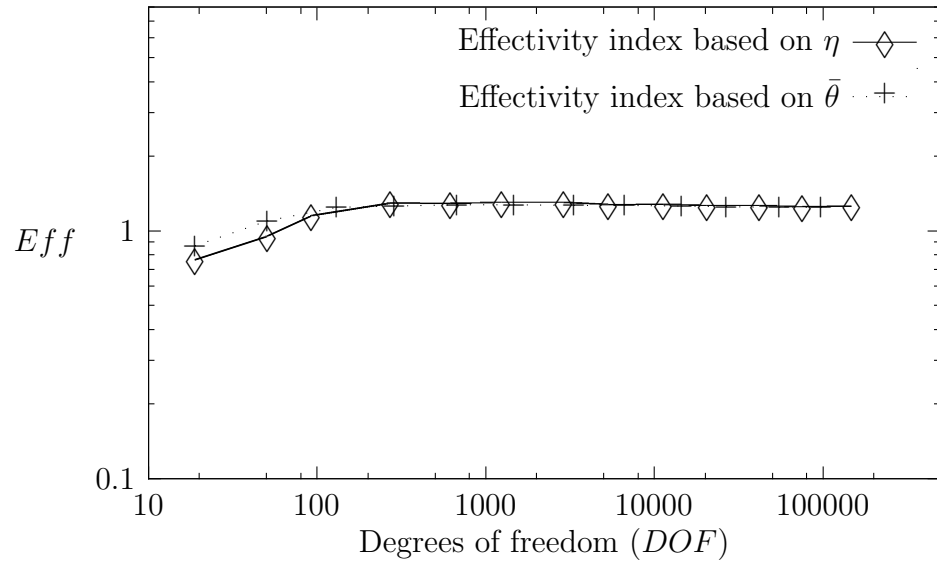


Figure 2: Effectivity indices vs DOF for adaptive refinements (Ex. 1, $\alpha = 1$).

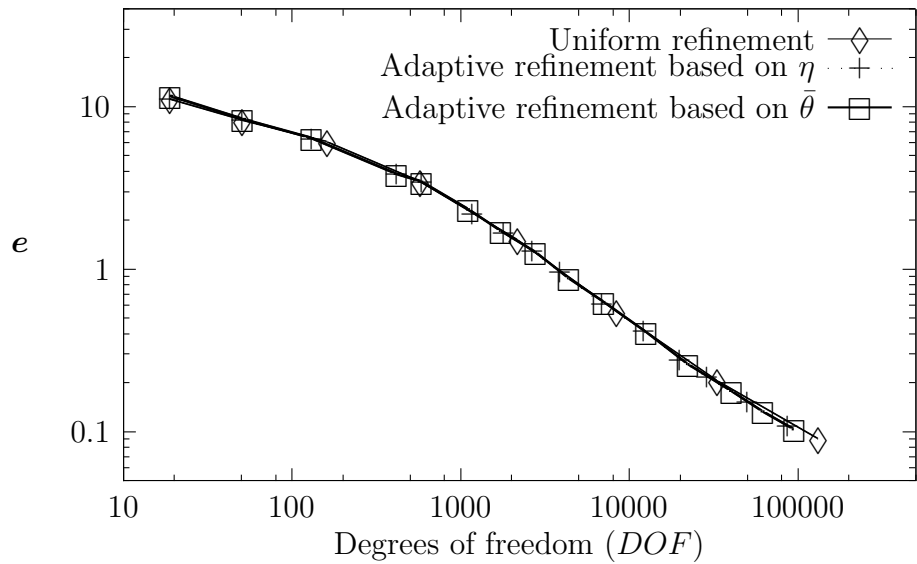


Figure 3: Total error e vs DOF for uniform and adaptive refinements (Ex. 1, $\alpha = 10^2$).

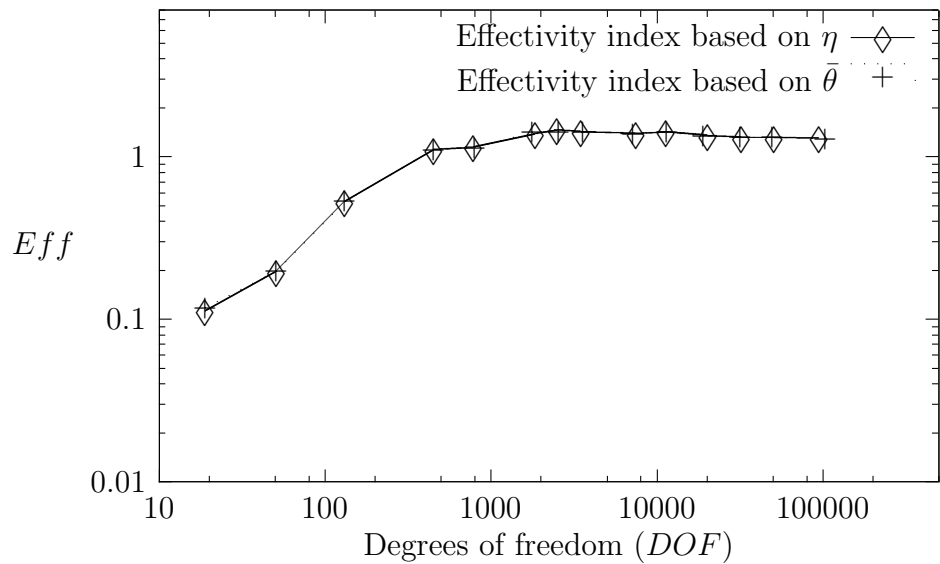


Figure 4: Effectivity indices vs DOF for adaptive refinements (Ex. 1, $\alpha = 10^2$).

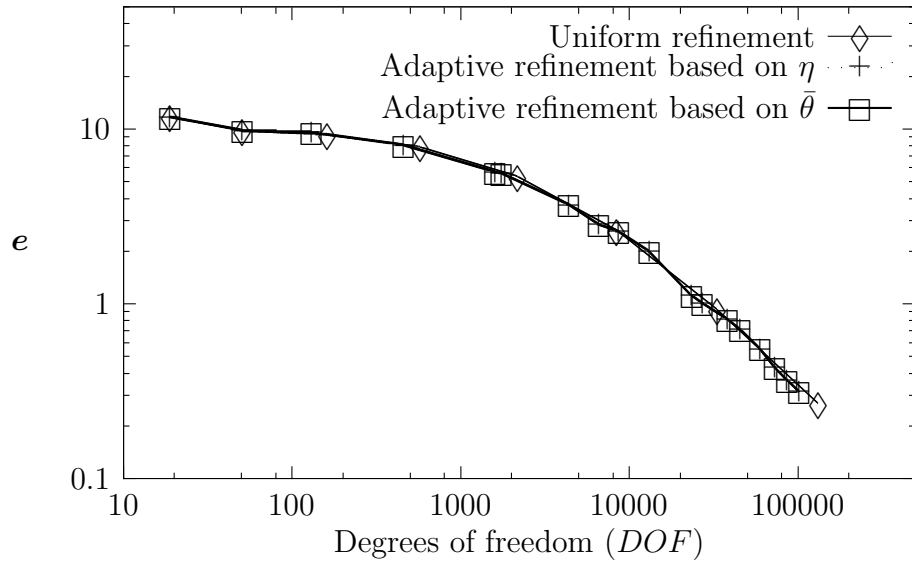


Figure 5: Total error e vs DOF for uniform and adaptive refinements (Ex. 1, $\alpha = 10^3$).

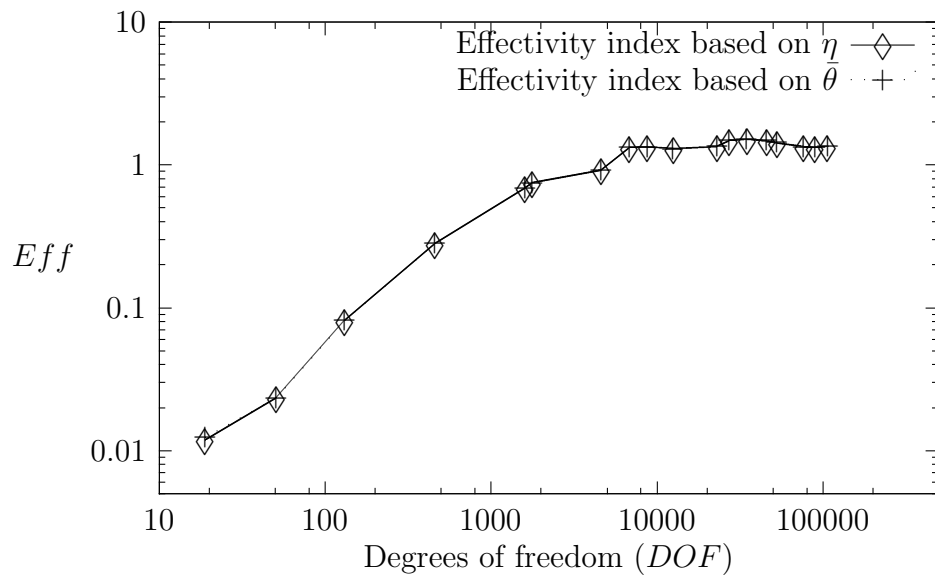


Figure 6: Effectivity indices vs DOF for adaptive refinements (Ex. 1, $\alpha = 10^3$).

<i>DOF</i>	$e(\mathbf{u})$	$r(\mathbf{u})$	$e(\boldsymbol{\sigma})$	$r(\boldsymbol{\sigma})$	e	r	e/η
43	1.410e-01	—	4.036e-01	—	4.275e-01	—	1.769e-04
119	5.543e-02	1.8337	2.528e-01	0.9195	2.588e-01	0.9864	1.542e-04
235	4.080e-02	0.9004	2.001e-01	0.6866	2.042e-01	0.6958	1.692e-04
351	4.066e-02	0.0176	1.854e-01	0.3802	1.898e-01	0.3647	1.972e-04
527	3.194e-02	1.1879	1.554e-01	0.8691	1.586e-01	0.8829	2.077e-04
763	2.419e-02	1.5016	1.252e-01	1.1668	1.275e-01	1.1797	2.070e-04
1183	1.576e-02	1.9555	9.927e-02	1.0590	1.005e-01	1.0859	2.048e-04
1813	1.330e-02	0.7942	8.208e-02	0.8909	8.315e-02	0.8885	2.121e-04
2733	8.240e-03	2.3327	6.289e-02	1.2972	6.343e-02	1.3189	2.013e-04
4151	6.645e-03	1.0291	5.253e-02	0.8615	5.295e-02	0.8642	2.065e-04
6633	4.496e-03	1.6676	3.967e-02	1.1988	3.992e-02	1.2054	1.983e-04
10411	3.422e-03	1.2107	3.230e-02	0.9116	3.248e-02	0.9151	2.020e-04
16103	2.870e-03	0.8058	2.693e-02	0.8335	2.708e-02	0.8331	2.086e-04
26043	1.868e-03	1.7882	2.018e-02	1.2001	2.027e-02	1.2059	1.990e-04
40377	1.484e-03	1.0474	1.655e-02	0.9061	1.661e-02	0.9073	2.038e-04
62469	1.215e-03	0.9195	1.372e-02	0.8577	1.378e-02	0.8581	2.084e-04
101935	7.577e-04	1.9273	1.021e-02	1.2068	1.024e-02	1.2115	1.987e-04
157463	6.095e-04	1.0008	8.393e-03	0.9021	8.415e-03	0.9026	2.037e-04
<i>DOF</i>	$e_0(\boldsymbol{\sigma}^d)$	$r_0(\boldsymbol{\sigma}^d)$	$e_0(p)$	$r_0(p)$	$e_0(\mathbf{u})$	$r_0(\mathbf{u})$	
43	2.167e-01	—	1.696e-01	—	4.797e-02	—	
119	1.359e-01	0.9160	9.289e-02	1.1834	1.807e-02	1.9184	
235	1.098e-01	0.6271	8.192e-02	0.3695	1.256e-02	1.0698	
351	1.063e-01	0.1634	8.311e-02	—	1.188e-02	0.2743	
527	8.981e-02	0.8286	7.159e-02	0.7348	7.790e-03	2.0783	
763	7.607e-02	0.8976	5.521e-02	1.4037	5.557e-03	1.8255	
1183	6.107e-02	1.0017	4.310e-02	1.1294	3.724e-03	1.8260	
1813	5.092e-02	0.8512	3.611e-02	0.8295	2.570e-03	1.7373	
2733	4.011e-02	1.1622	2.602e-02	1.5972	1.543e-03	2.4867	
4151	3.358e-02	0.8508	2.208e-02	0.7859	1.116e-03	1.5479	
6633	2.562e-02	1.1551	1.600e-02	1.3735	6.290e-04	2.4478	
10411	2.120e-02	0.8400	1.295e-02	0.9389	4.280e-04	1.7079	
16103	1.777e-02	0.8077	1.097e-02	0.7595	3.112e-04	1.4612	
26043	1.341e-02	1.1725	7.867e-03	1.3837	1.737e-04	2.4262	
40377	1.112e-02	0.8558	6.471e-03	0.8913	1.195e-04	1.7057	
62469	9.276e-03	0.8292	5.411e-03	0.8197	8.734e-05	1.4370	
101935	6.887e-03	1.2161	3.891e-03	1.3472	4.680e-05	2.5482	
157463	5.717e-03	0.8564	3.216e-03	0.8756	3.248e-05	1.6804	

Table 2: Ex. 2 with $\alpha = 10^{-4}$ and $\nu = 1$: adaptive refinement (based on η).

<i>DOF</i>	$e(\mathbf{u})$	$r(\mathbf{u})$	$e(\boldsymbol{\sigma})$	$r(\boldsymbol{\sigma})$	\mathbf{e}	r	e/η
43	1.278e-01	—	4.055e-01	—	4.252e-01	—	1.253e+00
119	5.281e-02	1.7369	2.536e-01	0.9223	2.590e-01	0.9737	1.204e+00
235	3.940e-02	0.8604	2.008e-01	0.6857	2.047e-01	0.6926	1.260e+00
419	3.065e-02	0.8688	1.611e-01	0.7624	1.640e-01	0.7662	1.314e+00
651	2.257e-02	1.3900	1.269e-01	1.0821	1.289e-01	1.0922	1.259e+00
1103	1.690e-02	1.0977	1.010e-01	0.8679	1.024e-01	0.8745	1.278e+00
1743	9.827e-03	2.3688	7.526e-02	1.2846	7.589e-02	1.3080	1.213e+00
2435	9.008e-03	0.5202	6.551e-02	0.8292	6.613e-02	0.8238	1.236e+00
4307	5.877e-03	1.4976	4.890e-02	1.0258	4.925e-02	1.0335	1.210e+00
6587	3.952e-03	1.8686	3.884e-02	1.0844	3.904e-02	1.0939	1.193e+00
9455	3.430e-03	0.7825	3.313e-02	0.8792	3.331e-02	0.8782	1.206e+00
17071	1.990e-03	1.8427	2.392e-02	1.1025	2.401e-02	1.1088	1.175e+00
25001	1.572e-03	1.2384	1.978e-02	0.9979	1.984e-02	0.9995	1.181e+00
38207	1.280e-03	0.9683	1.640e-02	0.8817	1.645e-02	0.8823	1.190e+00
65769	8.245e-04	1.6194	1.215e-02	1.1064	1.217e-02	1.1091	1.167e+00
97793	6.627e-04	1.1010	9.984e-03	0.9884	1.001e-02	0.9889	1.175e+00
153357	5.202e-04	1.0768	8.131e-03	0.9128	8.147e-03	0.9135	1.181e+00
<i>DOF</i>	$e_0(\boldsymbol{\sigma}^d)$	$r_0(\boldsymbol{\sigma}^d)$	$e_0(p)$	$r_0(p)$	$e_0(\mathbf{u})$	$r_0(\mathbf{u})$	
43	2.081e-01	—	1.746e-01	—	4.322e-02	—	
119	1.340e-01	0.8649	9.472e-02	1.2016	1.719e-02	1.8116	
235	1.084e-01	0.6220	8.325e-02	0.3792	1.228e-02	0.9887	
419	8.867e-02	0.6961	7.114e-02	0.5436	7.660e-03	1.6315	
651	7.480e-02	0.7723	5.249e-02	1.3799	5.329e-03	1.6474	
1103	6.100e-02	0.7735	4.243e-02	0.8077	3.650e-03	1.4357	
1743	4.563e-02	1.2685	2.914e-02	1.6414	1.937e-03	2.7695	
2435	4.123e-02	0.6078	2.642e-02	0.5879	1.587e-03	1.1930	
4307	3.103e-02	0.9969	1.881e-02	1.1911	9.204e-04	1.9095	
6587	2.456e-02	1.0992	1.460e-02	1.1928	5.627e-04	2.3163	
9455	2.163e-02	0.7044	1.279e-02	0.7321	4.451e-04	1.2971	
17071	1.526e-02	1.1804	8.706e-03	1.3018	2.159e-04	2.4485	
25001	1.277e-02	0.9349	7.308e-03	0.9176	1.531e-04	1.8023	
38207	1.080e-02	0.7875	6.192e-03	0.7819	1.130e-04	1.4313	
65769	7.806e-03	1.1969	4.368e-03	1.2844	5.610e-05	2.5794	
97793	6.494e-03	0.9278	3.662e-03	0.8892	3.986e-05	1.7226	
153357	5.361e-03	0.8526	3.024e-03	0.8506	2.789e-05	1.5882	

Table 3: Example 2 with $\alpha = 1$ and $\nu = 1$: adaptive refinement (based on η).

<i>DOF</i>	$e(\mathbf{u})$	$r(\mathbf{u})$	$e(\boldsymbol{\sigma})$	$r(\boldsymbol{\sigma})$	e	r	e/η
43	1.602e-02	—	1.010e+00	—	1.010e+00	—	3.636e+00
119	1.327e-02	0.3698	7.601e-01	0.5582	7.602e-01	0.5582	3.752e+00
235	1.124e-02	0.4880	6.000e-01	0.6952	6.001e-01	0.6952	3.636e+00
411	1.186e-02	—	5.168e-01	0.5340	5.170e-01	0.5337	3.607e+00
783	1.103e-02	0.2236	3.751e-01	0.9946	3.753e-01	0.9941	3.132e+00
1413	7.877e-03	1.1410	2.314e-01	1.6370	2.315e-01	1.6365	2.747e+00
1833	7.128e-03	0.7680	1.944e-01	1.3377	1.945e-01	1.3370	2.546e+00
3273	5.413e-03	0.9497	1.348e-01	1.2619	1.350e-01	1.2614	2.307e+00
5299	3.960e-03	1.2969	8.244e-02	2.0425	8.254e-02	2.0410	1.979e+00
7219	3.324e-03	1.1331	6.584e-02	1.4541	6.593e-02	1.4533	1.913e+00
11251	2.846e-03	0.7001	4.944e-02	1.2916	4.952e-02	1.2899	1.795e+00
18271	1.973e-03	1.5113	3.169e-02	1.8341	3.175e-02	1.8330	1.542e+00
25063	1.648e-03	1.1387	2.588e-02	1.2817	2.593e-02	1.2812	1.497e+00
41859	1.276e-03	0.9978	1.919e-02	1.1673	1.923e-02	1.1666	1.424e+00
66165	9.178e-04	1.4386	1.354e-02	1.5224	1.357e-02	1.5220	1.304e+00
95635	7.167e-04	1.3430	1.105e-02	1.1012	1.108e-02	1.1023	1.279e+00
160749	5.393e-04	1.0953	8.455e-03	1.0323	8.472e-03	1.0326	1.253e+00
<i>DOF</i>	$e_0(\boldsymbol{\sigma}^d)$	$r_0(\boldsymbol{\sigma}^d)$	$e_0(p)$	$r_0(p)$	$e_0(\mathbf{u})$	$r_0(\mathbf{u})$	
43	5.053e-02	—	3.162e-01	—	8.661e-03	—	
119	5.911e-02	—	2.335e-01	0.5960	6.589e-03	0.5373	
235	5.611e-02	0.1527	1.896e-01	0.6117	5.181e-03	0.7068	
411	5.401e-02	0.1366	1.731e-01	0.3263	4.385e-03	0.5966	
783	4.972e-02	0.2568	1.235e-01	1.0474	3.173e-03	1.0038	
1413	4.128e-02	0.6307	7.777e-02	1.5667	1.884e-03	1.7668	
1833	3.861e-02	0.5129	6.595e-02	1.2668	1.546e-03	1.5180	
3273	3.182e-02	0.6668	4.448e-02	1.3587	1.047e-03	1.3449	
5299	2.489e-02	1.0198	2.775e-02	1.9581	5.977e-04	2.3263	
7219	2.210e-02	0.7697	2.276e-02	1.2825	4.610e-04	1.6804	
11251	1.850e-02	0.8011	1.734e-02	1.2258	3.311e-04	1.4914	
18271	1.412e-02	1.1147	1.106e-02	1.8548	1.845e-04	2.4123	
25063	1.243e-02	0.8059	9.223e-03	1.1503	1.415e-04	1.6778	
41859	9.957e-03	0.8654	6.907e-03	1.1277	9.511e-05	1.5497	
66165	7.604e-03	1.1777	4.845e-03	1.5487	5.292e-05	2.5614	
95635	6.489e-03	0.8605	4.012e-03	1.0247	3.841e-05	1.7392	
160749	5.145e-03	0.8943	3.110e-03	0.9799	2.518e-05	1.6258	

Table 4: Example 2 with $\alpha = 10^2$ and $\nu = 1$: adaptive refinement (based on η).

<i>DOF</i>	$e(\mathbf{u})$	$r(\mathbf{u})$	$e(\boldsymbol{\sigma})$	$r(\boldsymbol{\sigma})$	e	r	e/η
43	6.571e-03	—	1.269e+00	—	1.269e+00	—	1.735e+00
131	4.000e-03	0.8913	1.240e+00	0.0415	1.240e+00	0.0415	4.606e+00
313	2.965e-03	0.6870	1.112e+00	0.2503	1.112e+00	0.2502	6.890e+00
499	2.576e-03	0.6041	1.021e+00	0.3638	1.021e+00	0.3638	7.887e+00
793	2.616e-03	—	9.397e-01	0.3593	9.397e-01	0.3593	7.597e+00
1709	2.697e-03	—	7.657e-01	0.5333	7.657e-01	0.5333	5.949e+00
4137	2.616e-03	0.0693	5.118e-01	0.9116	5.118e-01	0.9115	4.488e+00
7181	2.516e-03	0.1418	3.635e-01	1.2403	3.635e-01	1.2402	3.835e+00
12161	2.183e-03	0.5380	2.560e-01	1.3310	2.560e-01	1.3310	3.459e+00
16887	1.807e-03	1.1510	1.863e-01	1.9364	1.863e-01	1.9363	3.292e+00
22333	1.596e-03	0.8912	1.485e-01	1.6248	1.485e-01	1.6248	3.103e+00
34615	1.376e-03	0.6774	1.045e-01	1.6038	1.045e-01	1.6037	2.870e+00
42981	1.260e-03	0.8133	8.472e-02	1.9363	8.473e-02	1.9360	2.754e+00
57641	1.074e-03	1.0874	6.323e-02	1.9931	6.324e-02	1.9929	2.612e+00
69125	9.458e-04	1.3977	5.215e-02	2.1221	5.216e-02	2.1219	2.595e+00
75719	8.940e-04	1.2370	4.754e-02	2.0319	4.755e-02	2.0317	2.575e+00
99959	7.985e-04	0.8137	3.801e-02	1.6113	3.801e-02	1.6110	2.488e+00
121253	7.408e-04	0.7774	3.207e-02	1.7581	3.208e-02	1.7576	2.419e+00
167465	6.508e-04	0.8020	2.427e-02	1.7276	2.427e-02	1.7271	2.254e+00
<i>DOF</i>	$e_0(\boldsymbol{\sigma}^d)$	$r_0(\boldsymbol{\sigma}^d)$	$e_0(p)$	$r_0(p)$	$e_0(\mathbf{u})$	$r_0(\mathbf{u})$	
43	8.356e-03	—	3.692e-01	—	1.304e-03	—	
131	1.143e-02	—	3.694e-01	—	1.123e-03	0.2675	
313	1.516e-02	—	3.324e-01	0.2425	1.003e-03	0.2598	
499	1.663e-02	—	3.124e-01	0.2657	9.173e-04	0.3827	
793	1.739e-02	—	2.921e-01	0.2905	8.390e-04	0.3857	
1709	1.836e-02	—	2.349e-01	0.5674	6.806e-04	0.5450	
4137	1.756e-02	0.1005	1.513e-01	0.9961	4.509e-04	0.9315	
7181	1.623e-02	0.2857	1.062e-01	1.2818	3.161e-04	1.2884	
12161	1.413e-02	0.5255	7.403e-02	1.3707	2.205e-04	1.3665	
16887	1.259e-02	0.7016	5.411e-02	1.9093	1.592e-04	1.9830	
22333	1.139e-02	0.7216	4.346e-02	1.5689	1.256e-04	1.6980	
34615	9.614e-03	0.7716	2.995e-02	1.6982	8.768e-05	1.6407	
42981	8.693e-03	0.9313	2.435e-02	1.9131	7.053e-05	2.0105	
57641	7.584e-03	0.9296	1.804e-02	2.0455	5.224e-05	2.0453	
69125	6.946e-03	0.9684	1.515e-02	1.9228	4.289e-05	2.1721	
75719	6.655e-03	0.9384	1.392e-02	1.8518	3.901e-05	2.0806	
99959	5.920e-03	0.8432	1.115e-02	1.6007	3.095e-05	1.6655	
121253	5.414e-03	0.9251	9.454e-03	1.7055	2.586e-05	1.8633	
167465	4.663e-03	0.9246	7.166e-03	1.7162	1.915e-05	1.8588	

Table 5: Example 2 with $\alpha = 10^3$ and $\nu = 1$: adaptive refinement (based on η).

<i>DOF</i>	$e(\mathbf{u})$	$r(\mathbf{u})$	$e(\boldsymbol{\sigma})$	$r(\boldsymbol{\sigma})$	e	r	e/θ
43	1.410e-01	—	4.036e-01	—	4.275e-01	—	1.282e+00
119	5.543e-02	1.8337	2.528e-01	0.9195	2.588e-01	0.9864	1.187e+00
235	4.080e-02	0.9004	2.001e-01	0.6866	2.042e-01	0.6958	1.238e+00
419	3.132e-02	0.9149	1.605e-01	0.7637	1.635e-01	0.7695	1.295e+00
651	2.287e-02	1.4264	1.265e-01	1.0797	1.285e-01	1.0916	1.247e+00
1087	1.727e-02	1.0968	1.013e-01	0.8657	1.028e-01	0.8727	1.256e+00
1739	9.797e-03	2.4120	7.499e-02	1.2807	7.562e-02	1.3056	1.202e+00
2477	8.024e-03	1.1292	6.328e-02	0.9597	6.379e-02	0.9625	1.212e+00
4309	5.381e-03	1.4430	4.779e-02	1.0138	4.810e-02	1.0199	1.189e+00
6571	3.793e-03	1.6574	3.847e-02	1.0283	3.866e-02	1.0352	1.184e+00
9825	3.039e-03	1.1023	3.179e-02	0.9487	3.193e-02	0.9501	1.189e+00
16335	2.035e-03	1.5773	2.420e-02	1.0730	2.429e-02	1.0770	1.172e+00
24935	1.637e-03	1.0299	1.970e-02	0.9725	1.977e-02	0.9729	1.178e+00
39565	1.191e-03	1.3779	1.580e-02	0.9564	1.584e-02	0.9590	1.178e+00
62847	8.781e-04	1.3170	1.237e-02	1.0592	1.240e-02	1.0606	1.168e+00
98729	6.769e-04	1.1525	9.911e-03	0.9797	9.934e-03	0.9805	1.173e+00
156127	5.133e-04	1.2073	7.948e-03	0.9630	7.965e-03	0.9641	1.175e+00
<i>DOF</i>	$e_0(\boldsymbol{\sigma}^d)$	$r_0(\boldsymbol{\sigma}^d)$	$e_0(p)$	$r_0(p)$	$e_0(\mathbf{u})$	$r_0(\mathbf{u})$	
43	2.167e-01	—	1.696e-01	—	4.797e-02	—	
119	1.359e-01	0.9160	9.289e-02	1.1834	1.807e-02	1.9184	
235	1.098e-01	0.6271	8.192e-02	0.3695	1.256e-02	1.0698	
419	8.942e-02	0.7106	7.018e-02	0.5350	7.728e-03	1.6789	
651	7.518e-02	0.7872	5.182e-02	1.3764	5.346e-03	1.6724	
1087	6.166e-02	0.7738	4.233e-02	0.7890	3.684e-03	1.4527	
1739	4.548e-02	1.2953	2.890e-02	1.6243	1.917e-03	2.7798	
2477	3.992e-02	0.7369	2.481e-02	0.8620	1.479e-03	1.4661	
4309	3.010e-02	1.0202	1.813e-02	1.1336	8.529e-04	1.9891	
6571	2.418e-02	1.0379	1.443e-02	1.0820	5.360e-04	2.2015	
9825	2.059e-02	0.7988	1.204e-02	0.9013	3.976e-04	1.4848	
16335	1.543e-02	1.1361	8.861e-03	1.2054	2.185e-04	2.3560	
24935	1.267e-02	0.9320	7.303e-03	0.9143	1.496e-04	1.7914	
39565	1.029e-02	0.9017	5.878e-03	0.9406	1.008e-04	1.7104	
62847	7.960e-03	1.1081	4.492e-03	1.1623	5.848e-05	2.3526	
98729	6.415e-03	0.9553	3.634e-03	0.9380	3.869e-05	1.8295	
156127	5.198e-03	0.9187	2.932e-03	0.9371	2.577e-05	1.7724	

Table 6: Example 2 with $\alpha = 10^{-4}$ and $\nu = 1$: adaptive refinement (based on $\bar{\theta}$).

<i>DOF</i>	$e(\mathbf{u})$	$r(\mathbf{u})$	$e(\boldsymbol{\sigma})$	$r(\boldsymbol{\sigma})$	e	r	e/θ
43	1.278e-01	—	4.055e-01	—	4.252e-01	—	1.341e+00
119	5.281e-02	1.7369	2.536e-01	0.9223	2.590e-01	0.9737	1.202e+00
235	3.940e-02	0.8604	2.008e-01	0.6857	2.047e-01	0.6926	1.254e+00
419	3.065e-02	0.8688	1.611e-01	0.7624	1.640e-01	0.7662	1.307e+00
651	2.257e-02	1.3900	1.269e-01	1.0821	1.289e-01	1.0922	1.255e+00
1087	1.708e-02	1.0871	1.016e-01	0.8671	1.031e-01	0.8735	1.264e+00
1729	1.021e-02	2.2188	7.622e-02	1.2399	7.690e-02	1.2617	1.212e+00
2527	7.878e-03	1.3639	6.268e-02	1.0307	6.317e-02	1.0362	1.208e+00
4223	5.789e-03	1.2002	4.900e-02	0.9591	4.934e-02	0.9627	1.199e+00
6777	3.732e-03	1.8559	3.812e-02	1.0612	3.830e-02	1.0703	1.182e+00
9825	3.119e-03	0.9672	3.187e-02	0.9647	3.202e-02	0.9648	1.191e+00
16391	2.006e-03	1.7235	2.435e-02	1.0525	2.443e-02	1.0579	1.171e+00
25463	1.608e-03	1.0037	1.959e-02	0.9872	1.965e-02	0.9873	1.177e+00
39477	1.201e-03	1.3322	1.586e-02	0.9630	1.590e-02	0.9653	1.179e+00
62939	8.725e-04	1.3704	1.242e-02	1.0489	1.245e-02	1.0506	1.168e+00
100363	6.718e-04	1.1204	9.866e-03	0.9858	9.889e-03	0.9864	1.172e+00
155197	5.186e-04	1.1874	7.985e-03	0.9704	8.002e-03	0.9713	1.175e+00
<i>DOF</i>	$e_0(\boldsymbol{\sigma}^d)$	$r_0(\boldsymbol{\sigma}^d)$	$e_0(p)$	$r_0(p)$	$e_0(\mathbf{u})$	$r_0(\mathbf{u})$	
43	2.081e-01	—	1.746e-01	—	4.321e-02	—	
119	1.340e-01	0.8649	9.472e-02	1.2016	1.719e-02	1.8116	
235	1.084e-01	0.6220	8.325e-02	0.3792	1.228e-02	0.9887	
419	8.867e-02	0.6961	7.114e-02	0.5436	7.660e-03	1.6315	
651	7.480e-02	0.7723	5.249e-02	1.3799	5.329e-03	1.6474	
1087	6.141e-02	0.7693	4.280e-02	0.7965	3.674e-03	1.4507	
1729	4.608e-02	1.2373	2.983e-02	1.5558	1.987e-03	2.6486	
2527	3.963e-02	0.7946	2.438e-02	1.0639	1.454e-03	1.6457	
4223	3.098e-02	0.9600	1.886e-02	0.9984	9.185e-04	1.7892	
6777	2.397e-02	1.0836	1.421e-02	1.1983	5.275e-04	2.3451	
9825	2.069e-02	0.7937	1.208e-02	0.8744	4.011e-04	1.4753	
16391	1.559e-02	1.1062	8.905e-03	1.1913	2.243e-04	2.2706	
25463	1.260e-02	0.9668	7.229e-03	0.9466	1.485e-04	1.8714	
39477	1.036e-02	0.8940	5.899e-03	0.9275	1.026e-04	1.6890	
62939	8.022e-03	1.0951	4.503e-03	1.1582	5.984e-05	2.3107	
100363	6.390e-03	0.9746	3.607e-03	0.9510	3.853e-05	1.8871	
155197	5.240e-03	0.9106	2.944e-03	0.9320	2.646e-05	1.7250	

Table 7: Example 2 with $\alpha = 1$ and $\nu = 1$: adaptive refinement (based on $\bar{\theta}$).

<i>DOF</i>	$e(\mathbf{u})$	$r(\mathbf{u})$	$e(\boldsymbol{\sigma})$	$r(\boldsymbol{\sigma})$	e	r	e/θ
43	1.602e-02	—	1.010e+00	—	1.010e+00	—	3.640e+00
119	1.327e-02	0.3697	7.601e-01	0.5582	7.603e-01	0.5582	3.749e+00
235	1.124e-02	0.4880	6.000e-01	0.6952	6.001e-01	0.6952	3.629e+00
411	1.186e-02	—	5.168e-01	0.5340	5.170e-01	0.5337	3.597e+00
811	1.062e-02	0.3243	3.680e-01	0.9996	3.681e-01	0.9992	3.140e+00
1351	8.034e-03	1.0934	2.363e-01	1.7364	2.364e-01	1.7358	2.774e+00
1875	6.911e-03	0.9186	1.916e-01	1.2771	1.918e-01	1.2766	2.548e+00
3185	5.517e-03	0.8501	1.369e-01	1.2701	1.370e-01	1.2695	2.332e+00
5345	3.861e-03	1.3785	8.098e-02	2.0278	8.108e-02	2.0265	1.977e+00
7101	3.342e-03	1.0161	6.655e-02	1.3817	6.664e-02	1.3808	1.925e+00
11223	2.871e-03	0.6639	4.955e-02	1.2891	4.963e-02	1.2873	1.796e+00
18359	1.934e-03	1.6069	3.152e-02	1.8387	3.157e-02	1.8379	1.536e+00
24783	1.661e-03	1.0126	2.616e-02	1.2406	2.622e-02	1.2397	1.501e+00
42411	1.257e-03	1.0366	1.904e-02	1.1839	1.908e-02	1.1832	1.415e+00
66235	9.208e-04	1.3976	1.356e-02	1.5225	1.359e-02	1.5220	1.304e+00
95721	7.295e-04	1.2650	1.109e-02	1.0914	1.111e-02	1.0922	1.278e+00
162937	5.461e-04	1.0884	8.412e-03	1.0390	8.430e-03	1.0392	1.251e+00
<i>DOF</i>	$e_0(\boldsymbol{\sigma}^d)$	$r_0(\boldsymbol{\sigma}^d)$	$e_0(p)$	$r_0(p)$	$e_0(\mathbf{u})$	$r_0(\mathbf{u})$	
43	5.053e-02	—	3.162e-01	—	8.661e-03	—	
119	5.911e-02	—	2.335e-01	0.5960	6.589e-03	0.5373	
235	5.611e-02	0.1527	1.896e-01	0.6117	5.181e-03	0.7068	
411	5.401e-02	0.1366	1.731e-01	0.3263	4.385e-03	0.5966	
811	4.929e-02	0.2691	1.217e-01	1.0362	3.102e-03	1.0188	
1351	4.190e-02	0.6367	7.864e-02	1.7115	1.939e-03	1.8401	
1875	3.836e-02	0.5389	6.511e-02	1.1517	1.522e-03	1.4804	
3185	3.220e-02	0.6605	4.544e-02	1.3582	1.069e-03	1.3337	
5345	2.468e-02	1.0275	2.731e-02	1.9664	5.863e-04	2.3193	
7101	2.225e-02	0.7306	2.299e-02	1.2129	4.691e-04	1.5699	
11223	1.854e-02	0.7954	1.739e-02	1.2187	3.319e-04	1.5117	
18359	1.408e-02	1.1205	1.097e-02	1.8736	1.832e-04	2.4159	
24783	1.255e-02	0.7663	9.303e-03	1.0983	1.445e-04	1.5800	
42411	9.911e-03	0.8781	6.854e-03	1.1370	9.364e-05	1.6155	
66235	7.620e-03	1.1792	4.842e-03	1.5594	5.323e-05	2.5337	
95721	6.521e-03	0.8460	4.024e-03	1.0046	3.874e-05	1.7265	
162937	5.122e-03	0.9081	3.094e-03	0.9888	2.487e-05	1.6658	

Table 8: Example 2 with $\alpha = 10^2$ and $\nu = 1$: adaptive refinement (based on $\bar{\theta}$).

<i>DOF</i>	$e(\mathbf{u})$	$r(\mathbf{u})$	$e(\boldsymbol{\sigma})$	$r(\boldsymbol{\sigma})$	e	r	e/θ
43	6.571e-03	—	1.269e+00	—	1.269e+00	—	1.735e+00
131	4.000e-03	0.8913	1.240e+00	0.0415	1.240e+00	0.0415	4.606e+00
313	2.965e-03	0.6870	1.112e+00	0.2502	1.112e+00	0.2503	6.889e+00
499	2.576e-03	0.6041	1.021e+00	0.3638	1.021e+00	0.3638	7.886e+00
793	2.616e-03	—	9.397e-01	0.3593	9.397e-01	0.3593	7.596e+00
1709	2.697e-03	—	7.657e-01	0.5333	7.657e-01	0.5333	5.948e+00
4137	2.616e-03	0.0693	5.118e-01	0.9116	5.118e-01	0.9115	4.487e+00
7181	2.516e-03	0.1418	3.635e-01	1.2403	3.635e-01	1.2402	3.834e+00
12161	2.183e-03	0.5380	2.560e-01	1.3310	2.560e-01	1.3310	3.459e+00
16887	1.807e-03	1.1509	1.863e-01	1.9364	1.863e-01	1.9363	3.291e+00
22333	1.596e-03	0.8912	1.485e-01	1.6249	1.485e-01	1.6248	3.102e+00
34615	1.376e-03	0.6774	1.045e-01	1.6038	1.045e-01	1.6037	2.870e+00
42997	1.260e-03	0.8105	8.472e-02	1.9331	8.473e-02	1.9329	2.754e+00
57681	1.074e-03	1.0892	6.323e-02	1.9914	6.324e-02	1.9912	2.612e+00
69293	9.454e-04	1.3866	5.205e-02	2.1224	5.205e-02	2.1222	2.594e+00
75863	8.935e-04	1.2477	4.748e-02	2.0296	4.748e-02	2.0293	2.574e+00
99969	7.991e-04	0.8088	3.801e-02	1.6108	3.802e-02	1.6105	2.489e+00
121235	7.396e-04	0.8026	3.207e-02	1.7639	3.208e-02	1.7634	2.422e+00
166915	6.508e-04	0.8005	2.434e-02	1.7253	2.435e-02	1.7247	2.259e+00
<i>DOF</i>	$e_0(\boldsymbol{\sigma}^d)$	$r_0(\boldsymbol{\sigma}^d)$	$e_0(p)$	$r_0(p)$	$e_0(\mathbf{u})$	$r_0(\mathbf{u})$	
43	8.356e-03	—	3.692e-01	—	1.304e-03	—	
131	1.143e-02	—	3.694e-01	—	1.123e-03	0.2675	
313	1.516e-02	—	3.324e-01	0.2425	1.003e-03	0.2598	
499	1.663e-02	—	3.124e-01	0.2657	9.173e-04	0.3826	
793	1.739e-02	—	2.921e-01	0.2905	8.390e-04	0.3857	
1709	1.836e-02	—	2.349e-01	0.5674	6.806e-04	0.5450	
4137	1.756e-02	0.1005	1.513e-01	0.9961	4.509e-04	0.9315	
7181	1.623e-02	0.2857	1.062e-01	1.2818	3.161e-04	1.2884	
12161	1.413e-02	0.5255	7.403e-02	1.3708	2.205e-04	1.3665	
16887	1.259e-02	0.7016	5.411e-02	1.9093	1.592e-04	1.9830	
22333	1.139e-02	0.7216	4.346e-02	1.5689	1.256e-04	1.6980	
34615	9.614e-03	0.7716	2.996e-02	1.6982	8.767e-05	1.6407	
42997	8.692e-03	0.9302	2.435e-02	1.9091	7.053e-05	2.0071	
57681	7.583e-03	0.9293	1.804e-02	2.0425	5.223e-05	2.0443	
69293	6.938e-03	0.9698	1.512e-02	1.9253	4.280e-05	2.1729	
75863	6.650e-03	0.9356	1.391e-02	1.8447	3.895e-05	2.0787	
99969	5.920e-03	0.8432	1.115e-02	1.6024	3.097e-05	1.6615	
121235	5.415e-03	0.9244	9.455e-03	1.7104	2.586e-05	1.8701	
166915	4.670e-03	0.9258	7.196e-03	1.7080	1.922e-05	1.8565	

Table 9: Example 2 with $\alpha = 10^3$ and $\nu = 1$: adaptive refinement (based on $\bar{\theta}$).

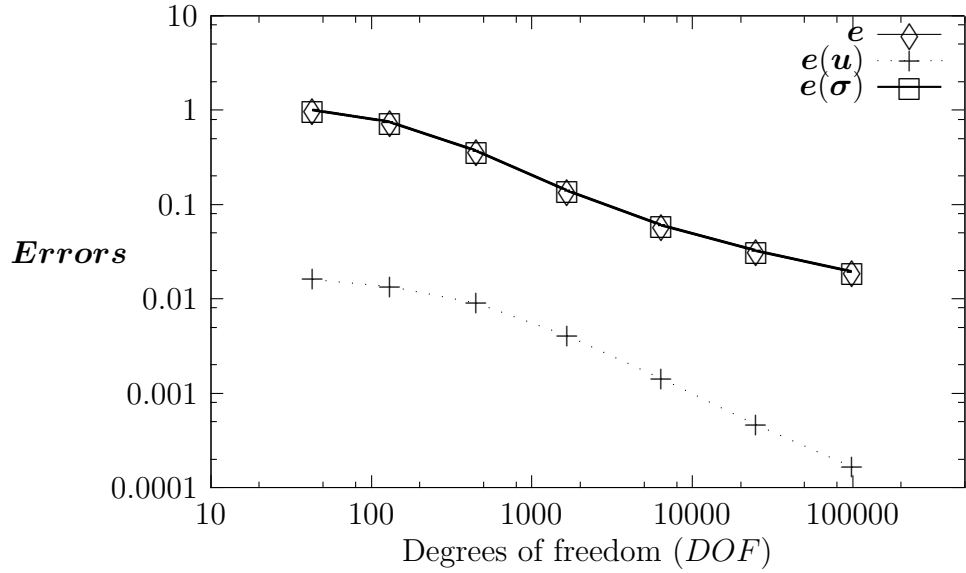


Figure 7: Individual errors $e(\mathbf{u})$ and $e(\boldsymbol{\sigma})$ vs DOF , for uniform refinement (Ex. 2, $\alpha = 10^2$).

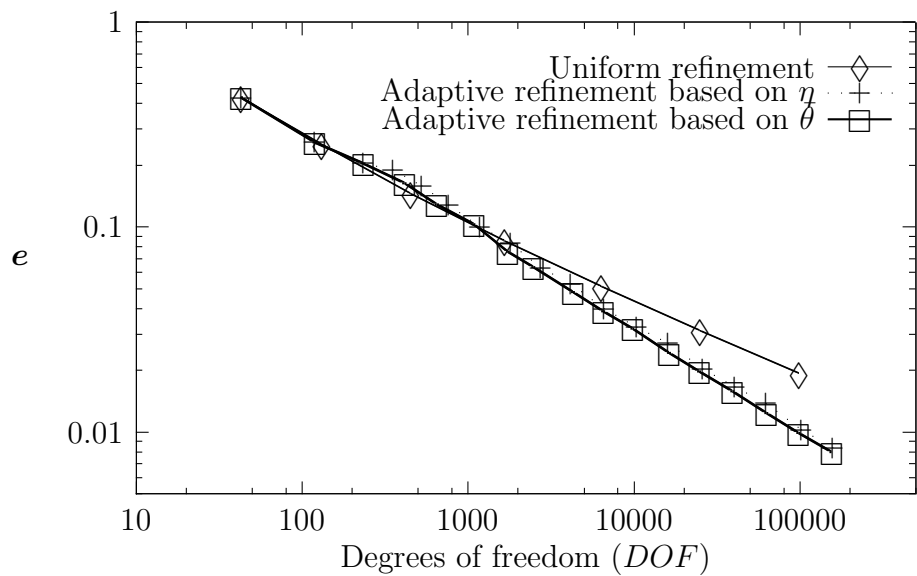


Figure 8: Total error e vs DOF for uniform and adaptive refinements (Ex. 2, $\alpha = 10^{-4}$).

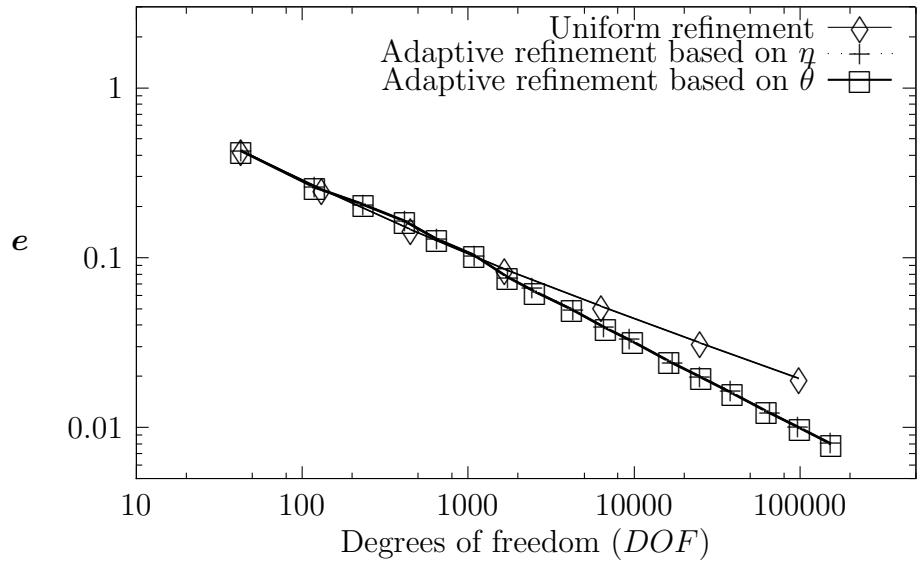


Figure 9: Total error e vs DOF for uniform and adaptive refinements (Ex. 2, $\alpha = 1$).

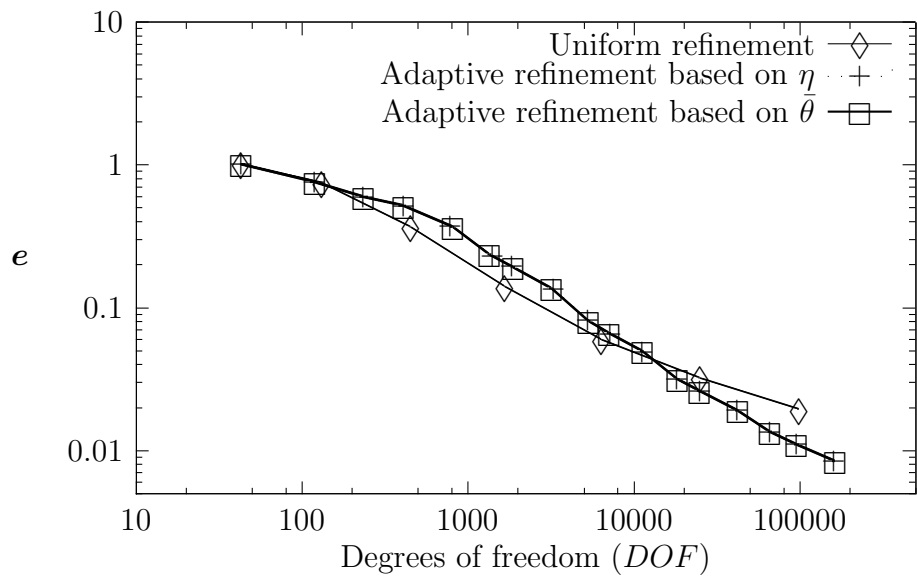


Figure 10: Total error e vs DOF for uniform and adaptive refinements (Ex. 2, $\alpha = 10^2$).

DOF	$e(\mathbf{u})$	$r(\mathbf{u})$	$e(\boldsymbol{\sigma})$	$r(\boldsymbol{\sigma})$	e	r	e/η
19	6.558e+00	—	1.923e+01	—	2.031e+01	—	1.206e+00
51	5.682e+00	0.2903	1.133e+01	1.0720	1.267e+01	0.9561	1.477e+00
163	3.542e+00	0.8136	6.628e+00	0.9221	7.515e+00	0.8992	1.783e+00
555	1.884e+00	1.0308	3.444e+00	1.0688	3.925e+00	1.0602	1.920e+00
2011	9.634e-01	1.0414	1.737e+00	1.0634	1.986e+00	1.0583	1.974e+00
7459	4.950e-01	1.0162	8.746e-01	1.0467	1.005e+00	1.0394	1.995e+00
20039	3.916e-01	0.4741	5.262e-01	1.0284	6.559e-01	0.8636	2.006e+00
29365	2.423e-01	2.5124	4.316e-01	1.0373	4.949e-01	1.4737	2.004e+00
78505	2.013e-01	0.3775	2.669e-01	0.9771	3.343e-01	0.7980	2.020e+00
115889	1.228e-01	2.5384	2.169e-01	1.0659	2.492e-01	1.5081	2.008e+00
DOF	$e_0(\boldsymbol{\sigma}^d)$	$r_0(\boldsymbol{\sigma}^d)$	$e_0(p)$	$r_0(p)$	$e_0(\mathbf{u})$	$r_0(\mathbf{u})$	
19	1.698e+00	—	1.459e+00	—	1.368e+00	—	
51	1.324e+00	0.5037	1.033e+00	0.6991	6.034e-01	1.6580	
163	7.387e-01	1.0046	5.220e-01	1.1749	2.150e-01	1.7759	
555	3.951e-01	1.0213	2.486e-01	1.2109	6.338e-02	1.9941	
2011	2.163e-01	0.9360	1.195e-01	1.1379	1.791e-02	1.9632	
7459	1.184e-01	0.9200	6.092e-02	1.0281	5.552e-03	1.7872	
20039	8.862e-02	0.5856	4.392e-02	0.6623	4.044e-03	0.6416	
29365	5.808e-02	2.2109	2.849e-02	2.2655	1.338e-03	5.7896	
78505	4.498e-02	0.5198	2.113e-02	0.6078	1.055e-03	0.4835	
115889	2.961e-02	2.1484	1.403e-02	2.1017	3.511e-04	5.6477	

Table 10: Example 3 with $\alpha = 10$ and $\nu = 0.5$: adaptive refinement (based on η).

<i>DOF</i>	$e(\mathbf{u})$	$r(\mathbf{u})$	$e(\boldsymbol{\sigma})$	$r(\boldsymbol{\sigma})$	e	r	e/θ
19	6.558e+00	—	1.923e+01	—	2.031e+01	—	6.311e-01
51	5.682e+00	0.2903	1.133e+01	1.0720	1.267e+01	0.9561	8.570e-01
163	3.542e+00	0.8136	6.628e+00	0.9221	7.515e+00	0.8992	1.001e+00
555	1.884e+00	1.0308	3.444e+00	1.0688	3.925e+00	1.0602	1.073e+00
2003	9.632e-01	1.0451	1.738e+00	1.0654	1.987e+00	1.0607	1.100e+00
6667	5.515e-01	0.9272	8.882e-01	1.1168	1.046e+00	1.0682	1.126e+00
12019	4.289e-01	0.8538	7.163e-01	0.7301	8.348e-01	0.7636	1.124e+00
26101	3.030e-01	0.8963	4.352e-01	1.2852	5.302e-01	1.1707	1.163e+00
48427	2.222e-01	1.0038	3.580e-01	0.6321	4.213e-01	0.7443	1.136e+00
100757	1.614e-01	0.8719	2.208e-01	1.3192	2.735e-01	1.1794	1.181e+00
<i>DOF</i>	$e_0(\boldsymbol{\sigma}^d)$	$r_0(\boldsymbol{\sigma}^d)$	$e_0(p)$	$r_0(p)$	$e_0(\mathbf{u})$	$r_0(\mathbf{u})$	
19	1.698e+00	—	1.459e+00	—	1.368e+00	—	
51	1.324e+00	0.5037	1.033e+00	0.6991	6.034e-01	1.6580	
163	7.387e-01	1.0046	5.220e-01	1.1749	2.150e-01	1.7759	
555	3.951e-01	1.0213	2.486e-01	1.2109	6.338e-02	1.9941	
2003	2.148e-01	0.9497	1.164e-01	1.1832	1.778e-02	1.9813	
6667	1.532e-01	0.5625	8.335e-02	0.5548	9.060e-03	1.1208	
12019	1.117e-01	1.0727	5.727e-02	1.2735	4.621e-03	2.2852	
26101	7.569e-02	1.0029	3.710e-02	1.1195	2.827e-03	1.2673	
48427	5.659e-02	0.9407	2.731e-02	0.9920	1.252e-03	2.6354	
100757	3.984e-02	0.9580	1.877e-02	1.0230	8.170e-04	1.1651	

Table 11: Example 3 with $\alpha = 10$ and $\nu = 0.5$: adaptive refinement (based on $\bar{\theta}$)

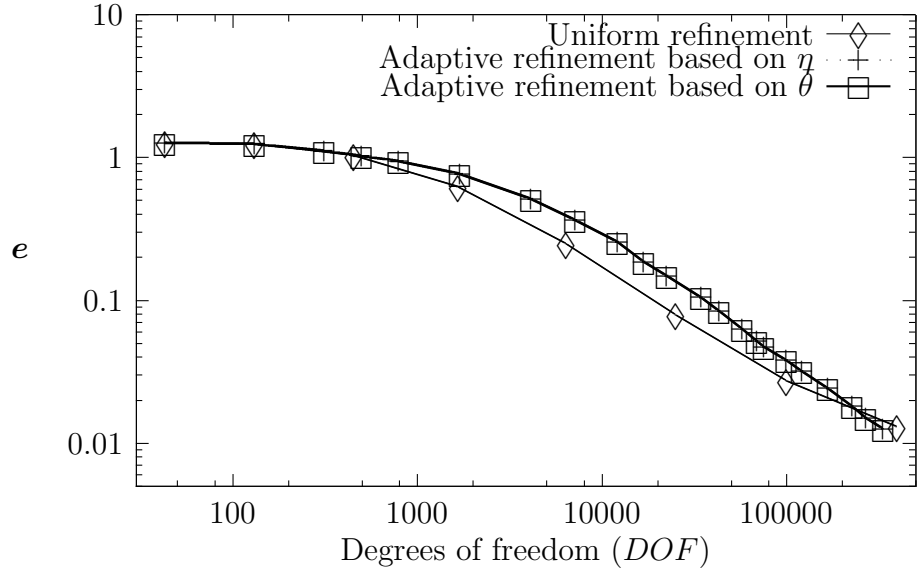


Figure 11: Total error e vs DOF for uniform and adaptive refinements (Ex. 2, $\alpha = 10^3$).

DOF	$e(\mathbf{u})$	$r(\mathbf{u})$	$e(\boldsymbol{\sigma})$	$r(\boldsymbol{\sigma})$	e	r	e/η
19	3.463e+01	—	1.769e+03	—	1.770e+03	—	1.518e-01
51	1.170e+02	—	1.343e+03	0.5591	1.348e+03	0.5518	1.668e-01
139	1.430e+02	—	1.071e+03	0.4504	1.081e+03	0.4403	2.377e-01
483	1.196e+02	0.2867	6.828e+02	0.7231	6.932e+02	0.7130	4.848e-01
1483	6.353e+01	1.1284	3.512e+02	1.1852	3.569e+02	1.1835	1.077e+00
3075	4.116e+01	1.1904	2.009e+02	1.5324	2.051e+02	1.5201	1.110e+00
5395	3.124e+01	0.9807	1.643e+02	0.7141	1.673e+02	0.7241	1.599e+00
13963	1.886e+01	1.0617	9.174e+01	1.2262	9.366e+01	1.2200	1.592e+00
19867	1.540e+01	1.1484	8.237e+01	0.6115	8.379e+01	0.6314	1.864e+00
45059	1.022e+01	1.0020	4.962e+01	1.2376	5.066e+01	1.2289	1.796e+00
60507	9.193e+00	0.7182	4.385e+01	0.8387	4.480e+01	0.8337	1.844e+00
153947	6.104e+00	0.8772	2.639e+01	1.0873	2.709e+01	1.0776	1.902e+00
DOF	$e_0(\boldsymbol{\sigma}^d)$	$r_0(\boldsymbol{\sigma}^d)$	$e_0(p)$	$r_0(p)$	$e_0(\mathbf{u})$	$r_0(\mathbf{u})$	
19	4.921e+01	—	3.942e+01	—	2.191e+01	—	
51	4.758e+01	0.0682	5.590e+01	—	1.503e+01	0.7632	
139	2.953e+01	0.9513	3.703e+01	0.8212	8.667e+00	1.0983	
483	2.180e+01	0.4876	1.748e+01	1.2058	2.833e+00	1.7954	
1483	1.171e+01	1.1084	7.657e+00	1.4712	6.213e-01	2.7051	
3075	7.801e+00	1.1129	1.094e+01	—	3.252e-01	1.7757	
5395	6.075e+00	0.8900	3.407e+00	4.1510	1.449e-01	2.8746	
13963	3.915e+00	0.9238	4.333e+00	—	7.764e-02	1.3130	
19867	3.092e+00	1.3396	1.634e+00	5.5314	3.813e-02	4.0328	
45059	2.343e+00	0.6776	1.581e+00	0.0801	2.541e-02	0.9909	
60507	1.937e+00	1.2896	1.321e+00	1.2190	1.987e-02	1.6698	
153947	1.358e+00	0.7611	7.249e-01	1.2855	9.239e-03	1.6399	

Table 12: Example 3 with $\alpha = 10^3$ and $\nu = 0.5$: adaptive refinement (based on η).

DOF	$e(\mathbf{u})$	$r(\mathbf{u})$	$e(\boldsymbol{\sigma})$	$r(\boldsymbol{\sigma})$	e	r	e/θ
19	3.463e+01	—	1.769e+03	—	1.770e+03	—	7.592e-02
51	1.170e+02	—	1.343e+03	0.5591	1.348e+03	0.5518	8.341e-02
139	1.430e+02	—	1.071e+03	0.4504	1.081e+03	0.4403	1.189e-01
483	1.196e+02	0.2867	6.828e+02	0.7231	6.932e+02	0.7130	2.426e-01
1483	6.353e+01	1.1284	3.512e+02	1.1852	3.569e+02	1.1835	5.404e-01
3075	4.116e+01	1.1904	2.009e+02	1.5324	2.051e+02	1.5201	5.574e-01
5155	3.122e+01	1.0707	1.648e+02	0.7661	1.677e+02	0.7775	8.065e-01
13723	1.881e+01	1.0347	9.267e+01	1.1761	9.456e+01	1.1709	8.062e-01
19619	1.538e+01	1.1263	8.220e+01	0.6704	8.363e+01	0.6871	9.445e-01
48929	1.002e+01	0.9383	4.743e+01	1.2038	4.847e+01	1.1937	9.020e-01
58673	9.216e+00	0.9181	4.410e+01	0.7997	4.506e+01	0.8047	9.391e-01
151723	6.103e+00	0.8676	2.677e+01	1.0507	2.746e+01	1.0424	9.663e-01
DOF	$e_0(\boldsymbol{\sigma}^d)$	$r_0(\boldsymbol{\sigma}^d)$	$e_0(p)$	$r_0(p)$	$e_0(\mathbf{u})$	$r_0(\mathbf{u})$	
19	4.921e+01	—	3.942e+01	—	2.191e+01	—	
51	4.758e+01	0.0682	5.590e+01	—	1.503e+01	0.7632	
139	2.953e+01	0.9513	3.703e+01	0.8212	8.667e+00	1.0983	
483	2.180e+01	0.4876	1.748e+01	1.2058	2.833e+00	1.7954	
1483	1.171e+01	1.1084	7.657e+00	1.4712	6.213e-01	2.7051	
3075	7.801e+00	1.1129	1.094e+01	—	3.252e-01	1.7757	
5155	6.113e+00	0.9441	3.567e+00	4.3386	1.456e-01	3.1094	
13723	3.971e+00	0.8810	4.679e+00	—	7.906e-02	1.2479	
19619	3.102e+00	1.3825	1.644e+00	5.8539	3.755e-02	4.1665	
48929	2.301e+00	0.6538	1.519e+00	0.1730	2.520e-02	0.8725	
58673	1.974e+00	1.6880	1.414e+00	0.7910	2.004e-02	2.5251	
151723	1.375e+00	0.7617	7.402e-01	1.3618	9.462e-03	1.5795	

Table 13: Example 3 with $\alpha = 10^3$ and $\nu = 0.5$: adaptive refinement (based on $\bar{\theta}$).

<i>DOF</i>	$e(\mathbf{u})$	$r(\mathbf{u})$	$e(\boldsymbol{\sigma})$	$r(\boldsymbol{\sigma})$	e	r	e/η
19	1.060e+03	—	1.957e+06	—	1.957e+06	—	5.629e-03
51	1.629e+03	—	1.369e+06	0.7242	1.369e+06	0.7242	5.058e-03
139	2.013e+03	—	9.448e+05	0.7397	9.448e+05	0.7397	4.634e-03
339	6.561e+03	—	6.856e+05	0.7193	6.856e+05	0.7192	4.789e-03
763	1.107e+04	—	5.212e+05	0.6758	5.213e+05	0.6754	5.739e-03
2595	1.117e+04	—	4.216e+05	0.3466	4.217e+05	0.3464	1.120e-02
4451	7.737e+03	1.3600	2.631e+05	1.7479	2.632e+05	1.7476	2.445e-02
12859	3.755e+03	1.3626	1.521e+05	1.0334	1.521e+05	1.0336	5.199e-02
15211	3.394e+03	1.2050	1.482e+05	0.3077	1.482e+05	0.3082	7.534e-02
37923	1.820e+03	1.3640	9.230e+04	1.0365	9.231e+04	1.0367	1.285e-01
53867	1.652e+03	0.5513	9.336e+04	—	9.337e+04	—	1.940e-01
147731	9.073e+02	1.1884	5.674e+04	0.9873	5.674e+04	0.9873	3.014e-01
<i>DOF</i>	$e_0(\boldsymbol{\sigma}^d)$	$r_0(\boldsymbol{\sigma}^d)$	$e_0(p)$	$r_0(p)$	$e_0(\mathbf{u})$	$r_0(\mathbf{u})$	
19	2.042e+03	—	1.636e+03	—	6.940e+02	—	
51	2.614e+03	—	4.054e+03	—	5.402e+02	0.5076	
139	2.884e+03	—	4.107e+03	—	4.069e+02	0.5649	
339	3.186e+03	—	2.898e+03	0.7823	2.858e+02	0.7930	
763	3.309e+03	—	2.945e+03	—	1.814e+02	1.1198	
2595	2.115e+03	0.7313	2.093e+03	0.5576	7.528e+01	1.4374	
4451	1.612e+03	1.0072	1.699e+03	0.7741	2.157e+01	4.6340	
12859	8.682e+02	1.1664	1.249e+03	0.5802	5.865e+00	2.4548	
15211	7.956e+02	1.0393	9.115e+02	3.7489	3.949e+00	4.7073	
37923	4.546e+02	1.2256	7.866e+02	0.3227	1.440e+00	2.2096	
53867	4.168e+02	0.4948	6.377e+02	1.1955	9.629e-01	2.2914	
147731	2.332e+02	1.1512	4.941e+02	0.5058	3.760e-01	1.8645	

Table 14: Example 3 with $\alpha = 10^6$ and $\nu = 0.5$: adaptive refinement (based on η).

<i>DOF</i>	$e(\mathbf{u})$	$r(\mathbf{u})$	$e(\boldsymbol{\sigma})$	$r(\boldsymbol{\sigma})$	e	r	e/θ
19	1.060e+03	—	1.957e+06	—	1.957e+06	—	2.815e-03
51	1.629e+03	—	1.369e+06	0.7242	1.369e+06	0.7242	2.529e-03
139	2.013e+03	—	9.448e+05	0.7397	9.448e+05	0.7397	2.317e-03
339	6.561e+03	—	6.856e+05	0.7193	6.856e+05	0.7192	2.394e-03
763	1.107e+04	—	5.212e+05	0.6758	5.213e+05	0.6754	2.869e-03
2595	1.117e+04	—	4.216e+05	0.3466	4.217e+05	0.3464	5.602e-03
4451	7.737e+03	1.3600	2.631e+05	1.7479	2.632e+05	1.7476	1.223e-02
12859	3.755e+03	1.3626	1.521e+05	1.0334	1.521e+05	1.0336	2.599e-02
15211	3.394e+03	1.2050	1.482e+05	0.3077	1.482e+05	0.3082	3.767e-02
37923	1.820e+03	1.3640	9.230e+04	1.0365	9.231e+04	1.0367	6.427e-02
53867	1.652e+03	0.5513	9.336e+04	—	9.337e+04	—	9.700e-02
147731	9.073e+02	1.1884	5.674e+04	0.9873	5.674e+04	0.9873	1.507e-01
<i>DOF</i>	$e_0(\boldsymbol{\sigma}^d)$	$r_0(\boldsymbol{\sigma}^d)$	$e_0(p)$	$r_0(p)$	$e_0(\mathbf{u})$	$r_0(\mathbf{u})$	
19	2.042e+03	—	1.636e+03	—	6.940e+02	—	
51	2.614e+03	—	4.054e+03	—	5.402e+02	0.5076	
139	2.884e+03	—	4.107e+03	—	4.069e+02	0.5649	
339	3.186e+03	—	2.898e+03	0.7823	2.858e+02	0.7930	
763	3.309e+03	—	2.945e+03	—	1.814e+02	1.1198	
2595	2.115e+03	0.7313	2.093e+03	0.5576	7.528e+01	1.4374	
4451	1.612e+03	1.0072	1.699e+03	0.7741	2.157e+01	4.6340	
12859	8.682e+02	1.1664	1.249e+03	0.5802	5.865e+00	2.4548	
15211	7.956e+02	1.0393	9.115e+02	3.7489	3.949e+00	4.7073	
37923	4.546e+02	1.2256	7.866e+02	0.3227	1.440e+00	2.2096	
53867	4.168e+02	0.4948	6.377e+02	1.1955	9.629e-01	2.2914	
147731	2.332e+02	1.1512	4.941e+02	0.5058	3.760e-01	1.8645	

Table 15: Example 3 with $\alpha = 10^6$ and $\nu = 0.5$: adaptive refinement (based on $\bar{\theta}$).

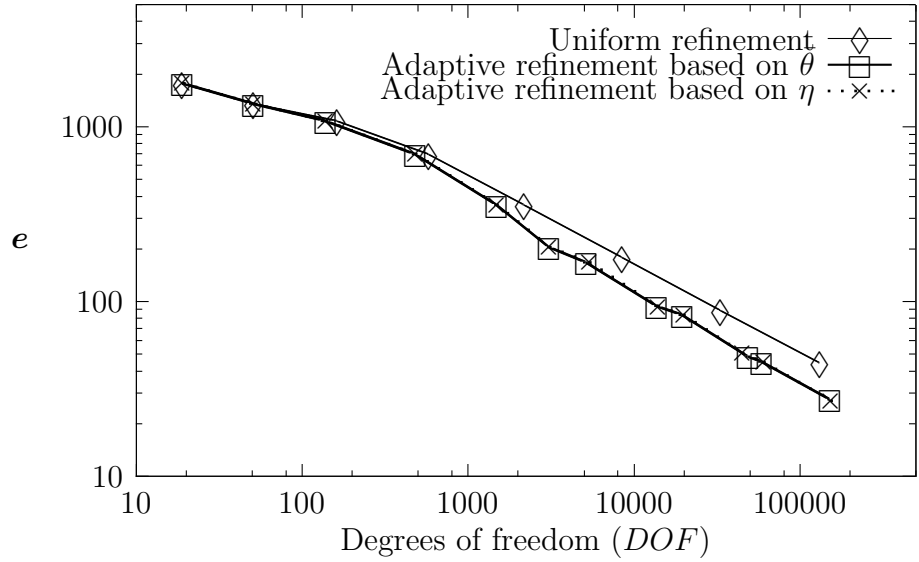


Figure 12: Total error e vs DOF for uniform and adaptive refinements (Ex. 3, $\alpha = 10^3$, $\nu = 0.5$).

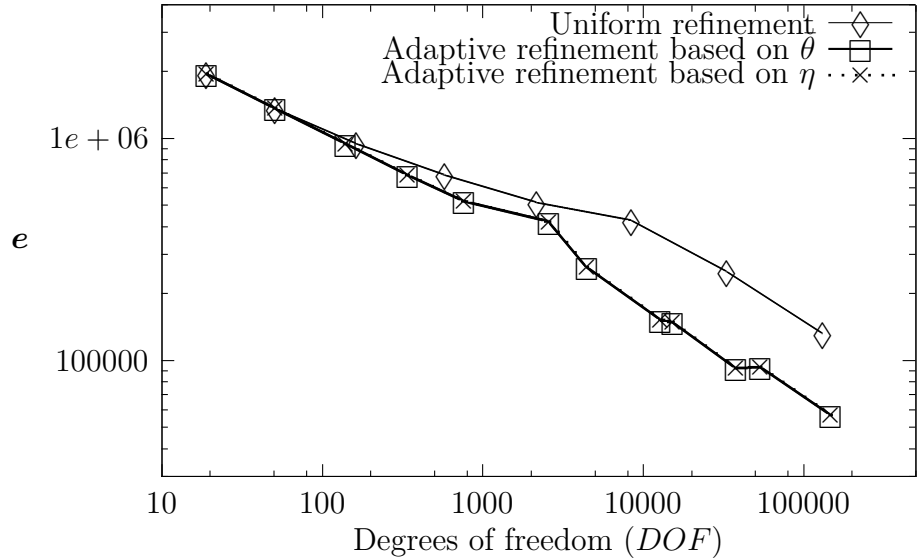


Figure 13: Total error e vs DOF for uniform and adaptive refinements (Ex. 3, $\alpha = 10^6$, $\nu = 0.5$).

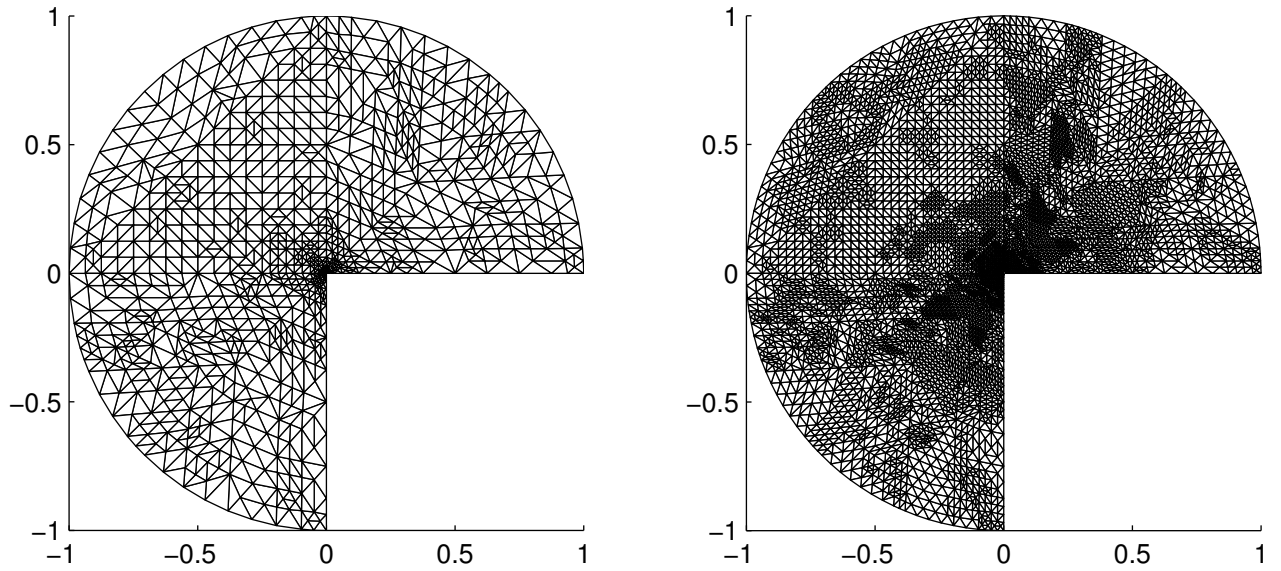


Figure 14: Ex. 2: Adapted meshes for η with 7219 (left) and 41859 (right) DOF ($\alpha = 10^2$).

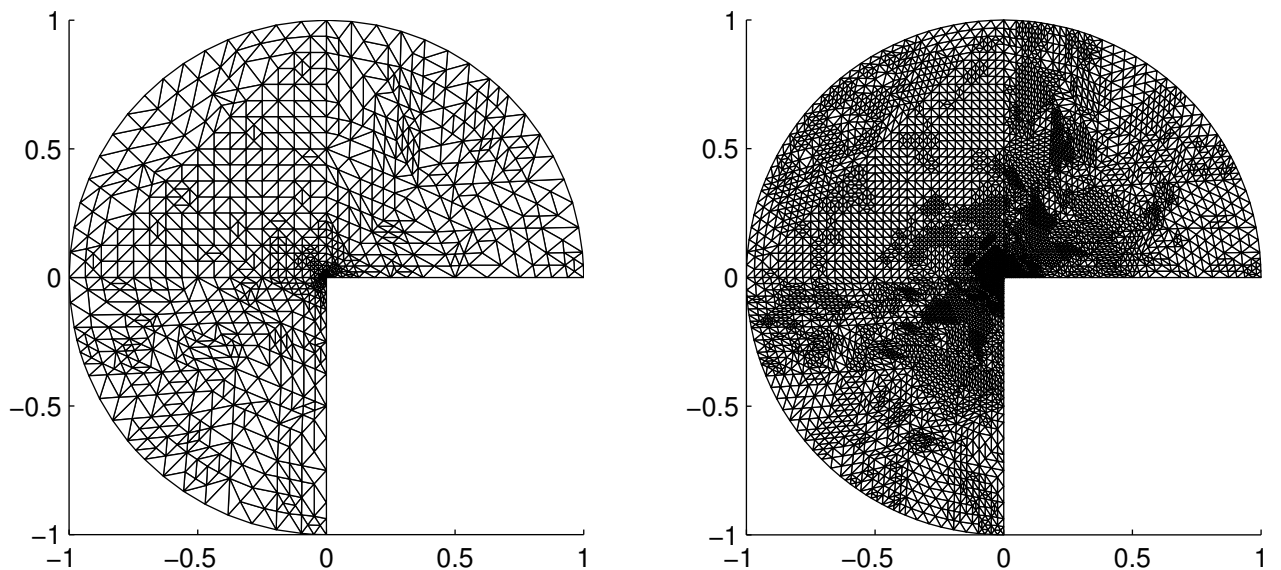


Figure 15: Ex. 2: Adapted meshes for $\bar{\theta}$ with 7101 (left) and 42411 (right) DOF ($\alpha = 10^2$).

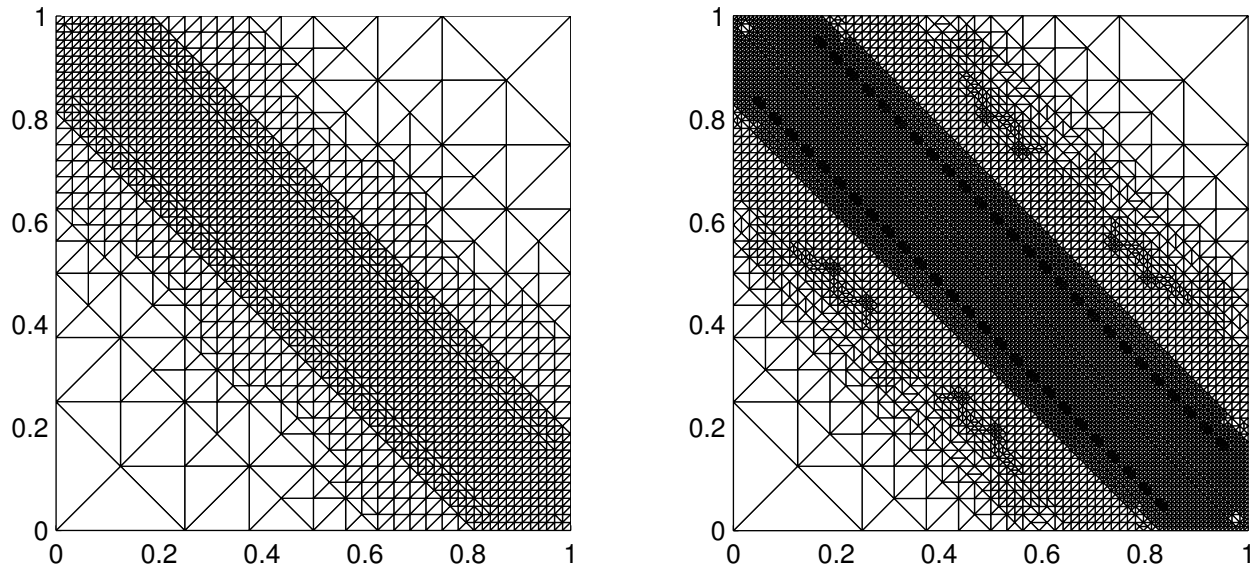


Figure 16: Ex. 3: Adapted meshes for η with 13963 (left) and 60507 (right) DOF ($\alpha = 10^3$).

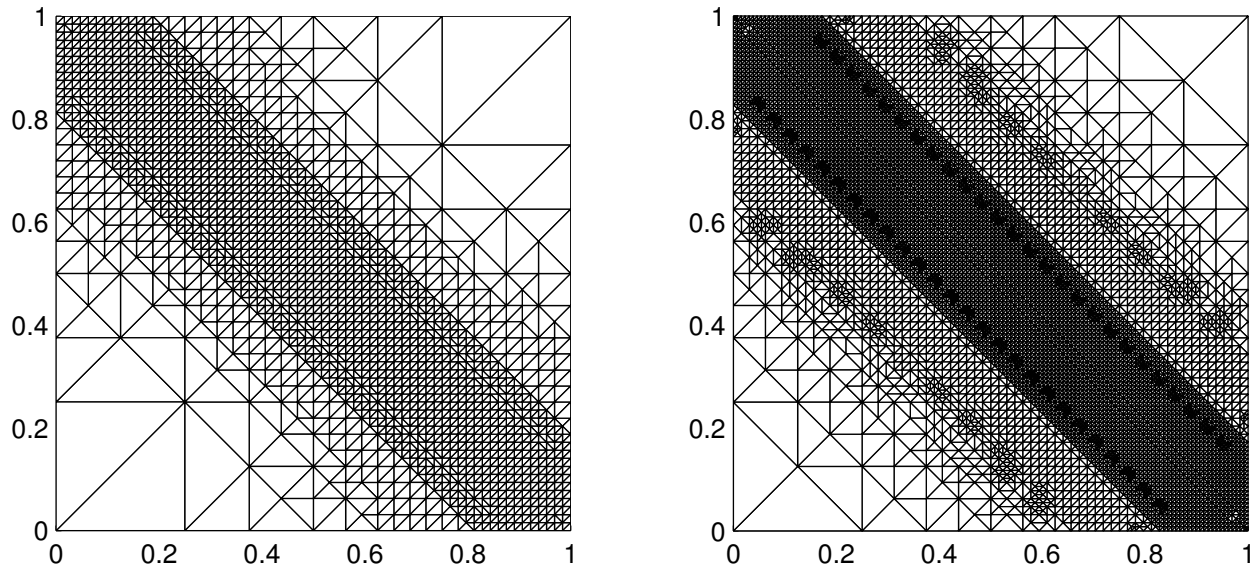


Figure 17: Ex. 3: Adapted meshes for $\bar{\theta}$ with 13723 (left) and 58673 (right) DOF ($\alpha = 10^3$).

References

- [1] S. AGMON, Lectures on Elliptic Boundary Value Problems. Van Nostrand, Princeton, New Jersey, 1965.
- [2] R. ARAYA, G. R. BARRENECHEA AND A. POZA, *An adaptive stabilized finite element method for a generalized Stokes problem*. Journal of Computational and Applied Mathematics, vol. 214, 2, pp. 457-479, (2008).
- [3] D.N. ARNOLD, *An interior penalty finite element method with discontinuous elements*. SIAM Jorunal on Numerical Analysis, vol. 19, 4, pp. 742-760, (1982).
- [4] G. R. BARRENECHEA AND F. VALENTIN, *An unusual stabilized finite element method for a generalized Stokes problem*. Numerische Mathematik, vol. 92, pp. 653-677, (2002).
- [5] T.P. BARRIOS, R. BUSTINZA, G. C. GARCÍA, AND E. HERNÁNDEZ, *On stabilized mixed methods for generalized Stokes problem based on the velocity-pseudostress formulation: A priori error estimates*. Computer Methods in Applied Mechanics and Engineering, vol. 237-240, pp. 78-87, (2012).
- [6] T.P. BARRIOS AND G.N. GATICA, *An augmented mixed finite element method with Lagrange multipliers: A priori and a posteriori error analyses*. Journal of Computational and Applied Mathematics, vol. 200, pp. 653-676, (2007).
- [7] F. BREZZI AND M. FORTIN, Mixed and Hybrid Finite Element Methods. Springer-Verlag, 1991.
- [8] E. BURMAN AND P. HANSBO, *Edge stabilization for the generalized Stokes problem: A continuous interior penalty method*. Computer Methods in Applied Mechanics and Engineering, vol. 195, pp. 2393-2410, (2006).
- [9] R. BUSTINZA, G.N. GATICA AND M. GONZÁLEZ, *A mixed finite element method for the generalized Stokes problem*. International Journal for Numerical Methods in Fluids, vol. 49, pp. 877-903, (2005).
- [10] Z. CAI, C. TONG, P.S. VASSILEVSKI AND C. WANG, *Mixed finite element methods for incompressible flow: Stationary Stokes equations*. Numerical Methods for Partial Differential Equations, vol. 26, pp. 957-978, (2010).
- [11] C. CALGARO AND J. LAMINIE, *On the Domain Decomposition Method for the Generalized Stokes problem with Continuous Pressure*. Numerical Methods for Partial Differential Equations, vol. 16, 1, pp. 84-106, (2000).

- [12] C. CARSTENSEN, *An a posteriori error estimate for a first-kind integral equation*, Mathematics of Computation, vol. 66 (217), pp. 139155, (1997).
- [13] P.G. CIARLET, The Finite Element Method for Elliptic Problems. North-Holland, 1978.
- [14] P. CLÉMENT, *Approximation by finite element functions using local regularisation*. RAIRO Modélisation Mathématique et Analyse Numérique, vol. 9, pp. 77-84, (1975).
- [15] G.N. GATICA: *Analysis of a new augmented mixed finite element method for linear elasticity allowing $RT_0-P_1-P_0$ approximations*. ESAIM: Mathematical Modelling and Numerical Analysis, vol. 40, 1, pp. 1-28, (2006).
- [16] G.N. GATICA, L. F. GATICA AND A. MARQUEZ, *Analysis of a pseudostress based mixed finite element method for Brinkman model of porous media flow*. Preprint 2012-02, Centro de investigación en Ingeniería Matemática, Universidad de Concepción, (2012).
- [17] G.N. GATICA, A. MÁRQUEZ AND M.A. SÁNCHEZ, *Analysis of a velocity-pressure-pseudostress formulation for the stationary Stokes equations*. Computer Methods in Applied Mechanics and Engineering, vol. 199, 17-20, pp. 1064-1079, (2010).
- [18] G.N. GATICA, A. MÁRQUEZ AND M.A. SÁNCHEZ, *Pseudostress-based mixed finite element methods for the Stokes problem in \mathbb{R}^n with Dirichlet boundary conditions. I: A priori error analysis*. Communications in Computational Physics, vol. 12, 1, pp. 109-134, (2012).
- [19] R. HIPTMAIR, *Finite elements in computational electromagnetism*. Acta Numerica, vol. 11, pp. 237-339, (2002).
- [20] S. REPIN AND R. STENBERG, *A posteriori error estimates for the generalized Stokes problem*. Journal of Mathematical Sciences, vol. 142, 1, pp. 1828-1843, (2007).
- [21] S. REPIN AND R. STENBERG, *Two-sided A posteriori estimates for a generalized Stokes problem*. Journal of Mathematical Sciences, vol. 159, 4, pp. 541-558, (2009).
- [22] J.E. ROBERTS AND J.-M. THOMAS, *Mixed and Hybrid Methods*. In: Handbook of Numerical Analysis, edited by P.G. Ciarlet and J.L. Lions, vol. II, Finite Element Methods (Part 1), 1991, North-Holland, Amsterdam.
- [23] R. VERFÜRTH, *A posteriori error estimation and adaptive mesh-refinement techniques*, J. Comput. Appl. Math., vol. 50, pp. 6783 (1994).
- [24] R. VERFÜRTH, A Review of a Posteriori Error Estimation and Adaptive Mesh-Refinement Techniques, Wiley-Teubner, Chichester, 1996.